

Quaternary Research

Implications of the geochemistry of L1LL1 (MIS2) loess in Poland for paleoenvironment and new normalizing values for loess-focused multi-elemental analyses --Manuscript Draft--

Manuscript Number:	QUA-23-72R2
Article Type:	Research Article
Keywords:	Elemental composition; Inductively Coupled Plasma; Late Pleistocene; Aeolian; Central Europe, PML - Polish Median Loess
Corresponding Author:	Jacek Skurzyński, Ph.D University of Wrocław Wrocław, Lower Silesian Voivodeship POLAND
First Author:	Jacek Skurzyński, Ph.D
Order of Authors:	Jacek Skurzyński, Ph.D Zdzisław Jary Kaja Fenn Frank Lehmkuhl Jerzy Raczyk Thomas Stevens Małgorzata Wieczorek
Abstract:	<p>Loess paleoenvironmental reconstructions on a (supra-)regional scale have recently gained much attention. Geochemistry comparisons in relation to a reference dataset such as UCC (Upper Continental Crust) data have helped understand the climatic and geomorphological conditions under which terrestrial sites have developed. However, UCC data differs from loess, thereby obscuring important features, and the existing "average loess" datasets also are not sufficient for modern investigations. In this study, we examine the youngest Polish loess (L1LL1=MIS2, ~26–15ka) for its suitability as a new, loess-focused reference dataset. A total of 89 samples from seven sites were analyzed, using Inductively Coupled Plasma spectrometry. The loess had assumedly been homogenized during transportation and/or sedimentary recycling (LaN/SmN=3.34–4.06, median 3.78; Eu/Eu*=0.46–0.66, median 0.55; GdN/YbN=1.08–1.49, median 1.26), and weakly affected by pre- or post-depositional weathering (CIA=53.64–69.12, median 57.69). The statistically significant differences between sites in elemental medians were mostly conditioned by variations in grain-size and in the "fresh" to "re-deposited" sediment ratio. Nonetheless, the overall geochemical composition homogeneity provided a basis for the estimation of Polish Median Loess (PML) data, as determined for 41 chemical elements. When used, PML data highlight differences between loess regions in Europe, thereby providing a tool for cross-continental comparisons.</p>

Dr Jacek Skurzyński
Department of Physical Geography
University of Wrocław
9th November 2023

Dear Editor,

We here submit the revised research article “**Implications of the geochemistry of L1LL1 (MIS2) loess in Poland for paleoenvironment and new normalizing values for loess-focused multi-elemental analyses**” for consideration by Quaternary Research. We confirm that this work is original and has not been published, nor is it under consideration for publication elsewhere.

This manuscript discuss the geochemical composition of Polish loess. We investigated a total number of 89 samples from seven sites, using Inductively Coupled Plasma – Emission Spectrometry (ICP-ES) and Inductively Coupled Plasma – Mass Spectrometry (ICP-MS) after sample fusion with lithium borate (in a furnace) and a cooled alloy dissolution with ACS grade nitric acid.

We show that the statistically significant differences in medians of elements between research sites were mostly conditioned by variations in grain-size distribution, and the proportion between "fresh" and "re-deposited" material. However, despite regional differences, investigated loess is strongly homogenized during transportation and/or sedimentary recycling, and not significantly affected by pre- or post-depositional processes.

We also report the estimation of new reference dataset (PML - Polish Median Loess) for multi-elemental analyses. The PML, determined for 41 chemical elements, is the first dataset which can replace the UCC as the normalizing dataset for loess.

As such, we believe that this manuscript is highly appropriate for submission to Quaternary Research and is of interest to a broad audience of geochemistry and palaeoenvironment researchers. We have no conflicts of interest to disclose.

Thank you for your consideration of this manuscript.

Yours faithfully
On behalf of the authors

Dr Jacek Skurzyński

1 **Implications of the geochemistry of L1LL1 (MIS2) loess in Poland for**
2 **paleoenvironment and new normalizing values for loess-focused multi-**
3 **elemental analyses**

4 **JACEK SKURZYŃSKI^a, ZDZISŁAW JARY^a, KAJA FENN^b, FRANK LEHMKUHL^c, JERZY**
5 **RACZYK^a, THOMAS STEVENS^d, MAŁGORZATA WIECZOREK^a.**

6
7 *^aInstitute of Geography and Regional Development, University of Wrocław, 1 Uniwersytecki Sqr.,*
8 *50-137 Wrocław, Poland*

9 *^bDepartment of Geography and Planning, University of Liverpool, Liverpool L69 7ZT, United*
10 *Kingdom*

11 *^cDepartment of Geography, Wüllnerstr. 5b, RWTH Aachen University, 52062 Aachen, Germany*

12 *^dDepartment of Earth Sciences, Uppsala University, Villavägen 16, Uppsala, 75236, Sweden*

13
14 Corresponding author: J. Skurzyński

15 e-mail: jacek.skurzynski@uwr.edu.pl

28 ABSTRACT

29 Loess paleoenvironmental reconstructions on a (supra-)regional scale have recently gained much attention.
30 Geochemistry comparisons in relation to a reference dataset such as UCC (Upper Continental Crust) data have
31 helped understand the climatic and geomorphological conditions under which terrestrial sites have developed.
32 However, UCC data differs from loess, thereby obscuring important features, and the existing “average loess”
33 datasets also are not sufficient for modern investigations. In this study, we examine the youngest Polish loess
34 (L1LL1 = MIS2, ~26 – 15 ka) for its suitability as a new, loess-focused reference dataset. A total of 89 samples
35 from seven sites were analyzed, using Inductively Coupled Plasma spectrometry. The loess had assumedly
36 been homogenized during transportation and/or sedimentary recycling ($La_N/Sm_N = 3.34 - 4.06$, median 3.78;
37 $Eu/Eu^* = 0.46 - 0.66$, median 0.55; $Gd_N/Yb_N = 1.08 - 1.49$, median 1.26), and weakly affected by pre- or
38 post-depositional weathering ($CIA = 53.64 - 69.12$, median 57.69). The statistically significant differences
39 between sites in elemental medians were mostly conditioned by variations in grain-size and in the "fresh" to
40 "re-deposited" sediment ratio. Nonetheless, the overall geochemical composition homogeneity provided a
41 basis for the estimation of Polish Median Loess (PML) data, as determined for 41 chemical elements. When
42 used, PML data highlight differences between loess regions in Europe, thereby providing a tool for cross-
43 continental comparisons.

44
45
46 **Keywords:** Elemental composition; Inductively Coupled Plasma; Late Pleistocene; Aeolian; Central Europe,
47 PML – Polish Median Loess.

56 INTRODUCTION

57 Loess is a clastic mineral dust deposit which occurs as wind-laid sheets (Smalley, Vita-Finzi 1968),
58 and is considered as one of the most investigated and best recognized terrestrial sediments (Schaetzl et al.,
59 2018; Waroszewski et al., 2021). Its bulk properties (such as granulometric or mineralogical composition)
60 show important variations with age, location, source area, topography, or depositional and post-depositional
61 weathering history (Rousseau et al., 2018; Lehmkuhl et al., 2016, 2021; Pötter et al., 2023). At the same time,
62 it is considered to be relatively homogeneous in terms of geochemical composition (Gallet et al., 1998; Wright,
63 1998; Tripathi and Rajamani, 1999; Újvári et al., 2008; Muhs, 2018; Fenn et al., 2022) due to its considerable
64 spread and mixing during transport. Consequently, its chemical composition was initially used mainly for the
65 stratigraphic location of the boundaries of individual layers (Sial et al., 2019), based on the assumption that
66 soil processes lead to the re-deposition of mobile and retention of immobile elements (Bugge et al. 2011).

67 Contemporary chemostratigraphic studies of loess focus on specific causes of stratigraphic and spatial
68 variation in chemical composition (Sial et al., 2019). However, they are limited by the lack of representative
69 sets of geochemical data from potential source areas (Bugge et al., 2008; Újvári et al., 2008). Some authors
70 have compared the chemical composition of loess with floodplain sediments (Bugge et al., 2008; Muhs and
71 Budahn, 2006; Újvári et al., 2014; Skurzyński et al., 2020) which represent the average composition of large
72 areas, and have been suggested as an immediate, up-wind, source of silty material (Smalley and Leach, 1978;
73 Hao et al., 2010; Schaetzl and Attig, 2013; Stevens et al., 2013; Obreht et al., 2015; Fenn et al., 2022;
74 Költringer et al., 2022). Other studies have compared the chemical signatures between loess-paleosol
75 stratigraphic sequences (e.g. Bugge et al., 2008; Újvári et al., 2008; Skurzyński et al., 2019; Pötter et al.,
76 2021). However, this approach may present different challenges due to the methodological differences of
77 determining the chemical composition (e.g., Miyazaki et al., 2016; Pötter et al., 2021), which may result in
78 significantly different values for the various chemical elements (Skurzyński and Fenn, 2022). One of the most
79 common comparative approaches is the use of normalized multi-element diagrams (e.g., Gallet et al., 1998;
80 Jahn et al., 2001; Bugge et al., 2008; Újvári et al., 2008, 2014; Rousseau et al., 2014; Campodonico et al.,
81 2019; Bosq et al. 2020; Skurzyński et al., 2020). These so-called spider diagrams (or spidergrams) are
82 constructed with respect to reference datasets such as the UCC (average composition of the Upper Continental
83 Crust; Condie, 1993; Taylor and McLennan, 1985; McLennan, 2001; Rudnick and Gao, 2003) or PAAS (Post-

84 Archaean Australian Average Shale; Taylor and McLennan, 1985), and identify deviations in composition
85 from the reference dataset (Rollinson, 2013). However, data reporting is poor, with some studies not providing
86 information on source of the normalization dataset (e.g. the version of the UCC).

87 Crucially, as the chemical composition of loess differs significantly from, e.g., the UCC or PAAS, it
88 causes strong positive or negative anomalies (e.g. Skurzyński et al., 2020) which obscures other changes
89 between individual samples. Consequently, attempts have been made to create a set of normalizing values
90 dedicated to loess, such as the Average Loess (Schnetger, 1992; presented later in the limited form as AVL¹
91 by Újvári et al., 2008) or Global Average Loess (GAL; Újvári et al., 2008). AVL was calculated using 24
92 samples taken from seven loess regions (Lukashev et al., 1965; Ebens et al., 1980; Taylor et al., 1983), and
93 GAL was based on the mean of 17 averages from 11 loess regions (244 samples, including these used for
94 AVL¹), with different quality of age control, and analyzed by different or even unreported methods (Lukashev
95 et al., 1965). Although GAL data constitute a significant contribution to the understanding of the geochemistry
96 of loess, they present data for only a limited number of chemical elements (even in relation to the original
97 Average Loess by Schnetger, 1992) and lack most of trace elements and rare earth elements (REE), which are
98 particularly important from a perspective of provenance studies, as major elements do not distinguish source
99 contributions (e.g., Fenn and Prud'homme, 2022; Skurzyński et al., 2020). Consequently, both GAL and other
100 existing "average chemical loess compositional data" are not sufficient for the comparative analysis of loess
101 from different parts of Europe or the world, and alternative reference data sets (such as UCC) are not suited
102 to the needs of loess research. Therefore, the old general assumption is valid - there is a need to introduce a
103 set of consistent and universally accepted normalizing values (Rock, 1987; Rudnick, 2013).

104 This study tackles this dilemma by presenting a new dataset dedicated to loess, based on samples
105 representing weakly weathered and relatively homogenous loess from areas with well-documented
106 chronostratigraphy, and measured with similar, reliable and precise methods. The loess cover of Poland was
107 chosen for this initial analysis, as it is thought to be representative of the whole Northern European Loess Belt.
108 It reflects contemporary and Pleistocene features of European climate: continental in the east and more oceanic
109 in the west (Cegła, 1972; Jersak, 1973; Maruszczak, 1991; Jary, 2007; Jary and Cizek, 2013), and is
110 lithologically diverse in relation to the latitudinal extent of the Pleistocene extra-glacial zone (Tutkovsky,
111 1899; Jahn, 1950). Consequently, we argue that the loess of eastern Poland shares many similarities (e.g. in

112 the granulometric composition) with the East European loess cover, whilst the western part is similar to the
113 western loesses (Maruszczak, 1991). Moreover, the Last Glacial Maximum loess in Poland (L1LL1 correlated
114 to MIS 2, ~26 - 15 ka) was demonstrated to have been strongly homogenized during transportation and/or
115 sedimentary recycling, and has not been significantly affected by pre- or post-depositional processes
116 (Skurzyński et al., 2020). We thus analyzed 89 loess samples from seven research sites, for major, trace and
117 rare earth element concentrations, to determine the factors influencing the chemical compositions of Polish
118 loess, and to propose new reference values of loess geochemical composition.

119 120 **RESEARCH AREA AND MATERIALS**

121 The loess cover of Poland relates to the very dynamic environment of Pleistocene glaciations (e.g.,
122 Tutkovsky, 1899; Jahn, 1950; Rousseau et al., 2014; Skurzyński et al., 2020) and was most likely sourced
123 from glacial deposits, as homogenized by meltwater rivers (Smalley et al., 2009, Badura et al., 2013;
124 Pańczyk et al., 2020; Baykal et al., 2021), with a variable proportion of local material (Pańczyk et al., 2020,
125 Baykal et al., 2021). The loess sites selected for sampling represent the full variability of the loess in Poland
126 (Fig. 1). They were divided into main and supplementary ones, considering the scope of geochemical analyses
127 and the accuracy of age control. We used the "universal" stratigraphical labelling system for this loess, first
128 introduced by Kukla and An (1989) and modified by Marković et al. (2008, 2015).

129 The L1LL1 loess units were sampled at these sites: Biały Kościół (Moska et al., 2019a), Złota (Moska
130 et al., 2018; Skurzyński et al., 2020) and Tyszowce (Moska et al., 2017; Skurzyński et al., 2019). These sites
131 have existing chronologies developed using Optically Stimulated Luminescence (OSL; Fig. 2) dating, and
132 they have been analyzed at high resolution for geochemistry. The main sites (representing the variability of
133 loess on the W-E axis, located at considerable distances from each other, and near the valleys of various large
134 rivers) represent the domain of the Northern European Loess Belt (domain II; Lehmkuhl et al., 2021) but each
135 likely formed under the different paleoenvironmental conditions (e.g., Maruszczak 1991). Biały Kościół
136 belongs to the subdomain IIb (Western European continental subdomain), and the rest of the sections to the
137 subdomain IIc (Central European continental subdomain) (Lehmkuhl et al., 2021). All of these loess sequences
138 were formed during the last interglacial-glacial (Fig. 2), although there are notable differences in the thickness
139 of individual loess covers (Fig. 2) which indicates different depositional rates. This further implies local

140 influences on the development of each profile on a sub-orbital scale, as suggested by Fenn et al. (2021). The
141 lithological features of the main research sites are also varied (Fig. 2). In the L1LL1 section at Biały Kościół
142 (especially in the lower part), weak tundra-gley soils, indications of periglacial deformation, or horizons of
143 initial gleying can be distinguished (Moska et al., 2019a). At Złota, the L1LL1 loess is more homogeneous,
144 although several horizons of initial gleying and/or deformation are also present (Fig. 2). The lowest parts are
145 deformed by cryogenic processes and show traces of slope redeposition (Moska et al., 2018; Skurzyński et al.,
146 2020). At Tyszowce, the L1LL1 loess can be as much as 14 m thick (Fig. 2). In the upper part (up to a depth
147 of ca. 5 m below ground level), sandy laminae are common (Fig. 2), suggesting short-term episodes of material
148 transport from the nearby Huczwa river valley (Skurzyński et al., 2019). Two generations of ice wedge
149 pseudomorphs in the L1LL1 loess indicate a double development cycle, and degradation of permafrost (Jary,
150 2007).

151 Four supplementary sites, i.e. Zaprężyn (Jary, 2007; Krawczyk et al., 2017; Skurzyński et al., 2017;
152 Zöller et al., 2022), Strzyżów (Moska et al., 2019b), Branice (Jary, 2007; Moska and Bluszcz, 2013) and
153 Odonów (Butrym, 1987; Jary, 2007) were also investigated to determine the spatial variability of the chemical
154 composition in the context of hetero- or homogeneity of the source material. The sites at Zaprężyn and
155 Strzyżów are located farther north than are Biały Kościół, Złota and Tyszowce, and the sections at Branice
156 and Odonów represent the southern parts of the loess in Poland (Fig. 1).

157 In this work 70 L1LL1 (MIS 2) samples were subject to geochemical analysis (Biały Kościół – 19,
158 Tyszowce – 32, Zaprężyn – 3, Strzyżów – 6, Odonów – 5, Branice – 5) following the methodology used
159 previously for Złota loess-paleosol sequence (Skurzyński et al., 2020). A further 19 published samples for
160 Złota's (Skurzyński et al., 2020) L1LL1 loess were also included, resulting in a total of 89 L1LL1 (MIS 2)
161 loess samples under study.

163 **METHODS**

164 The loess samples were collected in 2012 (Tyszowce, Złota and Zaprężyn), 2013 (Strzyżów), and 2018
165 (Biały Kościół). Samples from two of the sites (Branice and Odonów) are the result of earlier works (2002),
166 although the methodology used at that time did not significantly differ from that developed for the new
167 research sites (Jary, 2007). The air-dried samples were stored in plastic string bags.

168 Chemical analyses were performed in the commercial laboratory (Bureau Veritas, formerly ACME
169 labs; LF200 package) using Inductively Coupled Plasma – Emission Spectrometry (ICP-ES) and Inductively
170 Coupled Plasma – Mass Spectrometry (ICP-MS) after sample fusion with lithium borate (in a furnace) and a
171 cooled alloy dissolution with ACS grade nitric acid. Prior to the analysis, the material was passed through a
172 63 μm dry sieve to avoid the effect of grain-size differentiation on geochemical parameters values (e.g.,
173 Nesbitt and Young, 1982; Shao et al., 2012; Guan et al., 2016) and to minimize the influence of very local
174 sandy material (Skurzyński et al., 2019).

175 Analytical precision RSD (relative standard deviation) data were estimated separately for each of the
176 measurement series, based on several measurements (Table S1) of the certified STD SO-19 standard. The
177 average values for a given element were close to the expected value of the share of the analogous element in
178 the STD SO-19 standard, and the differences between the average values from individual series were usually
179 negligible (Table S1). The RSD is less than $\pm 5\%$ for most of the elements determined, and the variation
180 between measurement series is usually small (Table S1). For Cs, Ga, Hf and W, in some measurement series,
181 the RSD was less than $\pm 10\%$. For Be (which is not significant in the context of this paper), the RSD was more
182 variable, ranging from $\pm 4.79\%$ to $\pm 34.41\%$ in individual measurement series (Table S1).

183 The grain-size of the samples was determined by a Malvern Mastersizer 2000 laser grain-size analyzer,
184 which has a measurement range of 0.02–2000 μm with a precision of $\pm 1\%$. The refractive and absorption
185 indices used in the measurements were 1.544 and 0.1. Measurements were conducted after chemical pre-
186 treatment. The samples were first treated with H_2O_2 and 10% HCl to remove organic matter and carbonate,
187 respectively. Finally, the samples were dispersed with a 0.5 N sodium metaphosphate solution and
188 ultrasonicated for 10 min before measuring (e.g. Song et al., 2014; Skurzyński et al., 2019). The clay-silt
189 boundary assigned to the samples was 4 μm (e.g., Svensson et al., 2022), so the clay fraction may be
190 underestimated in relation to the data from publications utilizing higher clay-silt boundary, e.g. 8 μm (Konert
191 and Vandenberghe, 1997).

192 The concentrations of major (wt. %), trace elements and rare earths (ppm), as well as values of
193 geochemical parameters and granulometry, are shown in the Table S2. Basic, descriptive statistics (median,
194 average, minimum, maximum and standard deviation) are presented in Table S3. Throughout this article, the
195 median (instead of the mean) is used because most proportions of chemical elements (except Na_2O , K_2O ,

196 TiO₂, Ba, Sr, Y, and almost all of the rare earths are not normally distributed (tested using Shapiro-Wilk test;
197 Table S4). Consequently, non-parametric Kruskal-Wallis test (Table S4) and the Spearman correlation were
198 used for most analyses. The number of samples from supplementary sites was too limited for statistical
199 analysis, therefore comparison of the whole dataset was performed by the geochemical diagrams.

201 RESULTS

202 Chemical composition and granulometric background of the main research sites

203 The Kruskal-Wallis test (Table S4), in which the null hypothesis is that the medians of each group are
204 the same, showed that at least at one main research site the loess chemical composition differs significantly
205 from the others, by the median of practically each of the determined chemical elements (except MgO, P₂O₅,
206 MnO, Ni, and Zr).

207 Biały Kościół, as compared to the rest of main sites, is characterized by the highest median values for
208 most chemical elements (except SiO₂, CaO and Sr), and the highest minimum values for many major element
209 oxides (Al₂O₃, Fe₂O₃, K₂O, TiO₂, MnO) and all trace and rare earth elements (except Hf, Sr, and Zr). The
210 maximum values from Biały Kościół also are the highest in the entire dataset scale for most oxides (Al₂O₃,
211 Fe₂O₃, MgO, K₂O, and TiO₂) and trace elements (except Co, Ga, Hf, Nb, Sr, V, W, and Zr), and for all REEs
212 (Table S3). Further, it is the only profile where Ni was found in most of the samples (Table S2). This site is
213 characterized by the highest minimum values and the highest median of fine fractions (< 4 μm, 4-8 μm and 8-
214 16 μm), with the lowest median of medium (16-31 μm) and coarse (31-63 μm) silt. The median of sand (> 63
215 μm) also is the highest, but maximum value is the lowest in relation to the rest of the main research sites
216 (Table S3). The lower part (from a depth of approx. 4 m below ground level) is clearly enriched in fine
217 fractions (Table S2).

218 Złota is poorer in trace elements and REEs than is Biały Kościół, and richer than Tyszowce (Table
219 S3). However, the highest median of SiO₂, and (equals with Biały Kościół) Cr and W, were found in this
220 profile, as well as the highest minimum values of SiO₂, MgO, Na₂O, P₂O₅, Hf, W, and Zr (Table S3). In terms
221 of grain-size, Złota is characterized by the lowest median of fine fractions, and the only significant increase
222 of fine material was found in the lowest part of the L1LL1 loess, just above the L1SS1 soil (Fig. S1). The

223 median and minimum values of medium and coarse silt were the highest (Table S3). No significant enrichment
224 in the sand fraction was found (Fig. S1).

225 Loess at the Tyszowce site is the most depleted in the chemical components (if one considers median
226 values), with the exception of CaO and Sr, which reached the highest median values. However, the highest
227 maximum values of SiO₂, CaO, P₂O₅, MnO, Hf, Sr, Ta, W, Zr and Lu were found in relation to the rest of
228 main research sites (Table S3). Notably all the minimum values at Tyszowce (and the lowest minimum values
229 of the whole dataset) are in the upper, ~5-meters thick, sandy part of loess L1LL1 (Table S2). At Tyszowce,
230 the grain size variation is greater than in the other main sites (Fig. S1, Table S2). For example, the median
231 share of the sand fraction is the lowest (8.73%), with the lowest minimum value (2.09%) and the highest
232 maximum value (40.35%) - the standard deviation exceeds 9 (Table S3). Apart from the sand fraction, at
233 Tyszowce there is more coarse silt than at Biały Kościół, but less than at Złota. The share of fine fractions is
234 higher than at Złota, but lower than at Biały Kościół (Table S3). The fine material generally shows a clear
235 upward trend with depth, reaching maximum values in the lower part of the L1LL1 unit, but in several places
236 this trend is disturbed (Fig. S1).

237 **Chemical composition and granulometric background of the supplementary research sites**

238 Due to the limited number of samples from the supplementary sites Shepard's (1954) triangular
239 diagram, based on Wentworth's (1922) classification, was used to interpret grain sizes (Fig. S2). The use of
240 laser diffraction data could have caused the underestimation of the clay fraction (e.g. Konert and
241 Vandenberghe, 1997; Miller and Schaetzl, 2012; Bitelli et al., 2019), however it clearly shows the overall
242 diversity. The loess at Zaprężyn is enriched in the sand fraction in relation to the other supplementary research
243 sites (Fig. S2, Table S2). Loess from Odonów and Strzyżów show more “pure silt” granulometric
244 characteristics (Fig. S2). Loess at Strzyżów is not as variable in terms of grain size, although the samples
245 represent the part of L1LL1 loess of considerable thickness, from 3.20 to 9.30 m b.g.l. (Table S2). The loess
246 at Branice is distinguished by a significant amount of fine (<4 μm) fractions (Fig. S2, Table S2), with a low
247 share of coarse silt (31-63 μm) and sand (Table S2). The share of medium silt (16-31 μm) is comparable to
248 other supplementary sites (Table S2, Table S3). The results of the chemical composition of the supplementary
249 research sites, summarized in Table S2 and S3, will be discussed later, to avoid unnecessary repetitions.

DISCUSSION

Stratigraphic variability of the main research sites' chemical composition

All profiles show minor fluctuations and clear peaks of mobile (e.g. MgO, CaO or Fe₂O₃; Kabata-Pendias and Pendias, 1999) and immobile (e.g. Zr, Hf or Nb; Sheldon and Tabor, 2009) oxides and elements (Fig. 3-5; Table S2). This variation could be related to the changes in the mineralogical and/or grain-size composition, e.g. at 11.95 m depths of Tyszowce profile, where the sharp decrease in content of REEs was found (Fig. 5). This transition was followed by the peaks of Hf, Zr, U, and W (Fig. 4), which may be explained by additions different from the main mass of sediment (as suggested by the strong increase in the coarse silt; Fig. S1), e.g. from local sources or from the sediments enriched in resistant mineral phases.

The variability in chemical composition may be related to the post-depositional processes, such as bioturbation, gleying, and weak weathering (e.g. Kemp, 2001; Jeong et al., 2008; Mroczek, 2013). However, no clear influence of the initial tundra-gley soils on the chemical composition was found, except for a few horizons at Tyszowce (Fig. 3). Even decalcification, one of the first pedogenetic process taking place in loess (Liu, 1985; Jahn et al., 2001; Finke and Hutson, 2008), is not clearly indicated, based on elements associated with carbonates (e.g. CaO or Sr). Conversely the lower parts of the L1LL1 are generally enriched in oxides of the major elements (Fig. 3-5) such as aluminum (Al₂O₃). The Al₂O₃ is strongly positively related to the iron (Fe₂O₃; Spearman's correlation coefficient is 0.63 at Złota; 0.93 at Biały Kościół, and 0.99 at Tyszowce), which is one of the most mobile elements in humid-climate soils. Nonetheless, it has to be noted that iron mobility varies with conditions such as redox potential, the presence of organic matter or the type of mineral phases (Kabata-Pendias and Pendias, 1999). Similar tendencies to Al₂O₃ and Fe₂O₃ shows also TiO₂ (Fig. 3; e.g. at Tyszowce the Spearman's correlation coefficient between Al₂O₃ and TiO₂ is 0.81). This is of particular interest as TiO₂ is unlikely to migrate due to the very low solubility of its compounds (e.g. Sheldon and Tabor, 2009), and is consequently transported passively, in the form of primary minerals or in secondary products of weathering (Kabata-Pendias and Pendias, 1999). In reducing and acidic environments and in the presence of organic matter, TiO₂ is partially mobile, and enters the structure of clay minerals (Kabata-Pendias and Pendias, 1999). The increases in the contents of TiO₂, Al₂O₃ and Fe₂O₃ with depth (or simply in the deeper parts of the L1LL1 units) is likely driven by a greater share of e.g. clay minerals or amorphous hydroxides (Kabata-Pendias and Pendias, 1999; Reeder et al., 2006) in the source material (likely the older loess, eroded and re-

279 deposited e.g. from neighboring areas; e.g. Kemp, 2001; Jeong et al., 2008; Mroczek, 2013; Skurzyński et al.,
280 2020), and not by post-depositional changes.

281 Interpretations based on correlations between oxides (in percentages) seem reasonable, however they
282 may be faced with the closed-array compositional conundrum (Chayes, 1971; Templ et al., 2008; Rollinson,
283 2013; Andrews et al., 2023). That is, the increase in one oxide necessitates a decrease in at least one other
284 element, resulting in spurious negative correlations. Therefore, further analyses were based on geochemical
285 indicators and diagrams, which should not be significantly affected by the selective removal or enrichment
286 effect (e.g. Buggle et al., 2008). One of them is CIA, i.e. Chemical Index of Alteration (Nesbitt and Young,
287 1982), which is illustrated (Fig. S3-S5) on the A-CN-K diagrams (Nesbitt and Young, 1984).

288 The CIA for entire loess-paleosol sequence at Złota (including majority of samples taken from loess
289 L1LL2 and paleosol L1SS1, correlated to MIS 4 and MIS 3 respectively) ranges between 50 to 65 (Fig. S3;
290 Skurzyński et al., 2020) with only some samples experienced moderate weathering (65 to 85). These data
291 suggest that the site has undergone weak chemical weathering under a cold and dry climate (e.g., Song et al.,
292 2014) and periodic warm and moist paleoclimatic conditions for some of the soil samples (Fig. S3).
293 Considering only L1LL1 loess from Złota, the majority of samples are tightly clustered close to the CIA value
294 of 50, which is characteristic for unweathered crustal rocks (Nesbitt and Young, 1982, 1984). Additionally,
295 the lowermost part of the L1LL1 (6.35 – 6.75 m) is slightly more weathered (similarly to the L1LL2 unit)
296 (Fig. S3; Fig. 6).

297 At Biały Kościół, samples from the L1LL1 unit (Fig. S4; Fig. 6) are less clustered than at Złota (Fig.
298 S3; Fig. 6). The loess collected in the lowest part (4.73 - 5.3 m), above the L1SS1 soil, is the most weathered,
299 and the highest of all the samples (1.36 m) is with the lowest CIA value (Fig. S4). These data illustrate the
300 typical decreasing degree of chemical weathering upward the profile. However, there are some samples from
301 higher parts of the profile (1.55 m and to a lesser extent, 1.81 and 2.06 m) which are relatively more weathered
302 and enriched with K_2O (Fig. S4, Table S2). It may suggest the downward penetration of the effects of
303 pedogenesis (e.g., Han et al., 2019) and use of fertilizers, which are the main anthropogenic source of
304 potassium (e.g. Reeder et al., 2006). The least weathered samples are poorer in K_2O than other samples (Fig.
305 S4). In turn, the lower part of the profile (3.8 – 5.3 m) is also rich in K_2O , which may be related to the
306 enrichment in fine granulometric fractions (Table S2) - the very soluble simple cation K^+ , derived e.g. from

307 the weathered potassium feldspars, may be easily incorporated into the crystal lattice of clay minerals or
308 adsorbed on them (e.g. Reeder et al., 2006). As K-bearing mineral phases (such as potassium feldspars) are
309 quite resistant to chemical weathering (e.g. Wilson, 2004) the post-depositional processes cannot be the
310 dominant factor determining its variability in the investigated profile. Given the environmental conditions this
311 site experiences, feldspar breakdown is unlikely to be the key driver of potassium variability; a change in the
312 source material is more likely cause. However, taking into account the range of infiltration (from 2 to 5 m;
313 e.g. Tu et al., 2009; Zeng et al., 2016) and potential rapid transportation of rainwater through cracks
314 (Derbyshire, 2001), secondary enrichment cannot be ruled out.

315 At Tyszowce (Fig. S5) the samples taken from the deformation levels and/or initial soil horizons (e.g.
316 11.35 m, 12.95 m, or 14.6 m b.g.l.) clearly deviate from "the freshest" loess within the L1LL1 unit (e.g. 1.4
317 m, 8.15 m, or 9.55 m b.g.l.). These data may indicate changing paleoenvironmental conditions ("pure loess"
318 deposition vs post-depositional initial pedogenesis) during the formation of this very thick loess unit (e.g. Jary,
319 2007; Moska et al., 2017; Skurzyński et al., 2019). On the other hand, the lowest CIA values are associated
320 with layers enriched with sand (Fig. S5; Skurzyński et al., 2019), suggesting that the chemical composition
321 here is controlled by the mutual proportion of the finer and coarser materials.

323 **Factors controlling the spatial variability of Polish loess' chemical composition**

324 Most samples, representing the spatial variability of loess in Poland, are weakly weathered (Fig. 6).
325 Only loess samples from Branice oscillate around the CIA value of 65 (Fig. 6), resembling the data from the
326 L1SS1 soil at the Złota loess-paleosol sequence (Fig. S3). Considering that samples from Branice are
327 characterized by the finest grain size among Polish loess (Jary, 2007; Table S3), the effect of granulometric
328 sorting may be a better explanation than the different intensities of soil-forming processes (conditioned by
329 different features of the paleoclimate) for variability of CIA values. This conclusion is demonstrated by the
330 A-CN-K diagram, which reflects also the grain-size differentiation (Bugge et al., 2008) - the finest material
331 is the closest to the apex of the Al_2O_3 axis (Nesbitt et al., 1996) such as the highest CIA values (Nesbitt and
332 Young, 1984).

333 The highest values of CIA, and also the finest material, were found at Branice, and in the lowest parts
334 of the Biały Kościół (4.73 - 5.3 m), Tyszowce (14.6 m) and Złota (6.75 m) (Fig. 6). The remaining, even the

335 “freshest”, parts of L1LL1 at Biały Kościół (4.6 - 1.36 m) resemble the lower parts of L1LL1 at Tyszowce
336 (14.25 - 10.45 m) or at Złota (6.05, 6.35, 6.9 m), similarly to the loess from Odonów (Fig. 6). In turn, the
337 "freshest" loess in the whole dataset was found, in general terms, in the upper (and therefore the youngest)
338 parts of loess L1LL1 at Złota (0.55 - 5.6 m), Tyszowce (1 – 10 m and 11.75 - 11.95 m), and at the “northern”
339 sites i.e. Strzyżów and Zaprężyn (Fig. 6). The last one (Zaprężyn), located only approx. 60 km (straight-line
340 distance) towards NNE from the profile at Biały Kościół (Fig. 1), is particularly important in this context,
341 given that its weak weathering is likely not the direct result of different paleoclimatic conditions in relation to
342 the Biały Kościół. The better explanation may be so-called loess-cannibalism (Van Loon, 2006; Licht et al.,
343 2016), as a hiatus in loess deposition was found at Zaprężyn (from 56.8 ± 4.7 ka to 18.4 ± 1.2 ka; Zöller et al.,
344 2022). The “lacking” loess deflated from Zaprężyn theoretically could have been transported southwards and
345 re-deposited at Biały Kościół. It may further suggest that, similar to at Biały Kościół, the loess from “southern”
346 loess covers (Branice, Odonów), as well as the lowermost parts of the L1LL1 units from “eastern” loess-
347 paleosol sequences (Tyszowce and Złota) contain sediment eroded and reworked from paleosols or older loess
348 covers, and mixed with fresh, incoming dust (e.g. Mroczek 2013). Consequently, the varying proportions of
349 "older" and "fresher" material could explain the overall variability of the CIA values (Fig. 6), as the higher
350 supply of "fresh" material would have led to smaller chemical weathering values (e.g. Varga et al., 2011). In
351 this approach, the last phase of loess deposition in MIS 2 in the study area would have supplied the "fresh"
352 material to the “northern” profiles like Zaprężyn (since 18.4 ± 1.2 ka; Zöller et al., 2022) and Strzyżów
353 (substantial deposition since ~ 19 ka; Moska et al., 2019b). That supply of fresh sediment was likely provided
354 mostly from the north, given that loess with higher weathering values occurs in the south. Given the > 6 -meter
355 thick layer of loess L1LL1 (3.20 - 9.30 m) at Strzyżów, and the lack of differentiation of the low CIA values
356 there (Fig. 6), the supply was likely stable and substantial.

357 A “northern” source of the material is also suggested by the positive Zr and Hf anomalies (Fig. 7, Table
358 S2), which in Europe are commonly found for the periglacial loess (Rousseau et al., 2014 and the references
359 therein) and limited to material deposited near the Fenno-Scandinavian Ice Sheet (Scheib et al., 2014; Bosq et
360 al., 2020). This confirms the relationship of Polish loess to glacial deposits, as the enrichment with
361 elements related to the chemically resistant minerals, such as zircon (Zr and Hf), may be best attributed to the
362 removal of more weatherable minerals during the processes of glacial grinding and post-depositional leaching

363 in the sub- and proglacial environments of Poland (Lis and Pasieczna, 2006; Buggle et al., 2008). The data
364 also strengthen the previous premise about the relationship between the chemical and grain-size compositions
365 of the loess, as zircons are known to be preferentially concentrated in coarse silt and sand fractions in aeolian
366 sediments (Muhs and Bettis, 2000, Yang et al., 2006). The results further demonstrate that all samples
367 (collected both from the main and supplementary research sites) are arranged in accordance with the
368 sedimentary recycling trend line in the Zr/Sc vs Th/Sc diagram (Fig. 8), whilst the finest material is the most
369 depleted in zircons (Fig. 8).

370 We conclude that Polish loess can be considered to be generally unweathered sediment, with slight
371 variations in granulometry or weathering history. Therefore, the variability of chemical compositions is mostly
372 influenced by the enrichment and depletion of the silica, carbonates and secondary weathering products (Gallet
373 et al., 1998). In essence, the duration of post-depositional processes has not been long and intense enough to
374 mask the chemical signature of the loess parent material (Campodonico et al., 2019; Skurzyński et al., 2020).
375 Of course, admixtures of local material also may be important, e.g. the highest share of carbonates at Tyszowce
376 probably relates local bedrock, limestones (Maruszczak, 1991).

377 378 **General homogeneity of Polish loess' chemical composition**

379 The overall homogeneity of Polish loess is suggested by the very similar shape of the UCC-normalized
380 diagrams for all of the investigated sites (Fig. 7). Particularly important is the slight variation in REE curves,
381 as the magmatic or metamorphic rocks (the protolith of all the loess sediments) have a much greater diversity,
382 and the only way to “average” all these to a near-constant pattern is by recycling and mixing during at least
383 one cycle of sedimentary processes (Gallet et al., 1998). The statistically significant differences (Table S4) of
384 absolute abundances of chemical elements and oxides are not particularly important for the geochemical
385 indices, based on the trace element composition, e.g. Th/U (2.96–4.63; median 3.56), the lack of distinct Ce
386 anomaly (0.96–1.08; median 1.00), or the relatively stable values of La_N/Sm_N (3.34–4.06; median 3.78),
387 La_N/Yb_N (5.48–8.10; median 6.69) and Gd_N/Yb_N (1.08–1.49; median 1.26). These all suggest an
388 indistinguishable REE fractionation between “unweathered” and “weathered” loess, due to relatively greater
389 mobilization of HREE (heavy rare earths) than LREE (light rare earths). The significant weathering would

390 lead to a decrease in La_N/Sm_N values, and an increase in La_N/Yb_N and Gd_N/Yb_N values (Nesbitt, 1979; Hao et
391 al., 2010; Han et al., 2019; Skurzyński et al., 2020).

392 393 **PML – Polish Median Loess**

394 The weakly weathered (Fig. 6) Polish loess is geochemically homogeneous, relative to published data
395 on loess around the world (e.g., Pye, 1984; Rousseau et al., 2014; Bosq et al., 2020). Thus, it may be of
396 importance for paleoenvironmental interpretations, as trace elements and rare earths are widely used to infer
397 the provenance of sediments (Li et al., 2021; Shi et al., 2023), but the differences may be relatively minor, and
398 for the different loess deposits e.g. the REE patterns in the normalized diagrams are hardly distinguishable
399 (Guo, 2010). For example, the HREE patterns may be a good overall indicator of loess diversity in Europe
400 (Skurzyński et al., 2020). Thus, Gd_N/Yb_N values of Polish loess were tested against the background of samples
401 from various European loess areas (Fig. 9). To avoid comparing differences related to adopted research
402 methodology (Skurzyński and Fenn, 2022) only studies which used similar approaches were utilized
403 (Rousseau et al., 2014; Bosq et al., 2020). Additionally, a cross-analysis of the Gd_N/Yb_N was carried out (for
404 Tyszowce and Złota: this study vs Bosq et al., 2020; and for Surduk: Bosq et al., 2020 vs Rousseau et al.,
405 2014). For the loess sample from Tyszowce analyzed by Bosq et al. (2020), the value of Gd_N/Yb_N was 1.13
406 (this study: median 1.18, min. 1.08, max. 1.35) and for Złota, it was 1.17 (this study: median 1.26, min. 1.18,
407 max. 1.34). The Gd_N/Yb_N for the Surduk profile (located in Serbia) was 1.43 according to Bosq et al. (2020),
408 and 1.55 according to Rousseau et al. (2014). For Polish loess, the values of Gd_N/Yb_N are visibly lower than
409 the loess in Surduk, which is understandable, as these loess deposits have different sources. Similarly, low
410 values like in Polish loess were found (Fig. 9) e.g. in the English Channel, Ukraine (Stayky, Korshiv), E
411 Germany (Ostrau, Zeuchfeld) or Aquitaine (Pomarez). Even for the most weathered Polish loess (Branice;
412 Fig. 9) the median of Gd_N/Yb_N is lower than in the publication by Bosq et al. (2020), comparable to the median
413 from Rousseau et al. (2014).

414 As evidenced, even relatively small differences in the values of the appropriately chosen parameters
415 between Polish loess and loess from other regions can be detected, and therefore infer important information
416 about the source of the material. However, these kinds of minor differences are often imperceptible due to the
417 UCC normalization, which is very common in the literature. This set of chemical data is unsuited to the

418 specificity of loess. For this reason, many elements create very clear positive or negative anomalies on the
419 UCC-normalized diagrams (Fig. 7). Therefore, a set of normalization data dedicated to loess could be used,
420 such as AVL¹ (Schnetger, 1992; modified by Újvári et al., 2008) or GAL (Újvári et al., 2008). However, these
421 normalizing sets are based on the results obtained using variable methods, from samples representing diverse
422 worldwide loess regions, and showing values for limited number of elements (most trace elements and REEs
423 are omitted). An additional complication is the fact that even in a not very large group of "loess normalization
424 data sets", the same "average loess" may be presented in different scope and under different names. A good
425 example is the "average loess" introduced by Schnetger (1992) and cited later as AVL¹ by Újvári et al (2008)
426 in the way limited to the selected chemical elements. This may cause some confusion, so the name AVL¹ has
427 been consistently used in this work (Újvári et al., 2008), however, Table 1 presents the complete set of
428 elements from the original "average loess" (Schnetger, 1992). The relevant information can be found in the
429 caption of Table 1.

430 Therefore, we propose a new parameter (PML – Polish Median Loess), based on data obtained by same
431 methods, from one loess region with a homogeneous and “fresh” chemical composition, i.e., Poland.
432 Moreover, the PML dataset represents a near complete range of variability of chemical composition of loess
433 deposited at a similar time (MIS 2, as shown by numerous OSL ages) although differing in granulometric
434 composition. The PML is based on medians of individual elements, not average values – for this reason, it is
435 insensitive to outlier values remained in the data set (the paleoenvironmental information related to them was
436 not lost).

437 The PML is determined in wt.%, on a volatile-free basis, for oxides of major elements, and in ppm for
438 trace elements and rare earths. Its values are clearly different from previously published average loess
439 compositions (GAL and AVL¹; Table 1), but show some similar trends to them, such as higher values of
440 elements related to chemically and mechanically resistant mineral phases (e.g. SiO₂, Hf, Zr), in relation to the
441 UCC (Table 1). The differences between PML and UCC (Table 1) seem more important, because the latter is
442 widely used. We next tested the new loess-dedicated normalization data set against two loess samples from
443 different regions (Ukraine and Serbia; Bosq et al., 2020) and compared with UCC-normalized data via
444 multielemental spidergrams (Fig. 10).

445 The UCC-normalization of the Korshiv (Ukraine) section shows numerous positive and negative
446 anomalies, while PML-normalization illustrates that loess from Korshiv is only slightly enriched in MnO,
447 MgO, CaO and Sr, as compared to Polish loess (Fig. 10). Conversely, Serbian loess has higher values of
448 almost all elements and oxides in relation to the Polish loess - it is much more visible than in the case of UCC-
449 normalization (Fig. 10). This suggests that the use of PML may highlight even the barely noticeable
450 differences between loess regions in Europe. It may also facilitate the cross-continental comparative analysis
451 of loess geochemical compositions. We note that, for this type of analysis, the focus has traditionally been on
452 Asian and North American loess (e.g., Muhs, 2018).

453 By developing the PML we hope that other regional reference datasets (for e.g. China, USA,
454 Argentina) will be next developed, using similar methods, which will allow for further geochemical
455 comparisons. Until then, PML remains a reliable and comprehensive dataset for loess normalization
456 elsewhere.

457

458 **CONCLUSIONS**

459 The geochemical composition of the youngest (MIS 2) Polish loess units (L1LL1) are clearly
460 differentiated in vertical profiles. However, the classic chemostratigraphy, based on the analysis of the
461 variability of individual elements (or their correlations) with depth, is not always suitable for loess deposited
462 in a dynamic periglacial environment. The more effective way to examine this loess is to use geochemical
463 diagrams, which should not be significantly affected by the selective removal or enrichment effect, and by the
464 effect of closed-array compositional conundrum, which may result in spurious negative correlations.

465 The analysis of chemical weathering in the loess showed that the most weathered sites are located in
466 the southern part of Poland, as well as the lowest parts of the sections in the north. The "freshest" loess was
467 found, in general terms, in the upper (and therefore the youngest) parts of the L1LL1 loess at Złota, Tyszowce,
468 Strzyżów and Zaprężyn. The comparatively weak weathering data for loess at Zaprężyn changes the earlier
469 assumptions about the clear division of the Polish loess area into more weathered loess of western Poland and
470 relatively fresh loess of eastern Poland. The profiles located in the northern part of the research area (both in
471 the east and in the west) are much "fresher" than the profiles representing the southern sector of Poland. The
472 most reasonable explanation seems to be the deflation and transportation of the older material southwards and

473 later depositing it, for example, at the Biały Kościół or Branice areas. As a consequence, there is no "older"
474 material more to the north, e.g. at Zaprzężyn, where the "fresh" material was deposited.

475 Nonetheless, despite statistically significant differences in the degree of chemical weathering, as well
476 as in the other geochemical parameters and indices, the general homogeneity (or the well-mixed nature) of
477 Polish loess is clearly visible and has been demonstrated for each of the research sites. The loess is relatively
478 "fresh", strongly mixed and homogenized during transportation and/or sedimentary recycling, and not
479 significantly affected by post-depositional processes, or the admixtures of the local material.

480 The overall homogeneity of the Polish loess studied here has allowed for the calculation of a new,
481 loess-normalizing dataset named PML (Polish Median Loess). These data may be of particular importance for
482 comparative analyses of loess from different parts of the world. The PML may also constitute the basis for
483 further work on a pan-European or even global reference dataset - in this case, the condition is to maintain
484 rigor in the research methodology used and in the selection of research sites and samples.

485 486 **ACKNOWLEDGMENTS**

487 The geochemical research was performed under the National Science Centre project No.
488 2017/27/N/ST10/01208 entitled "Stratigraphic and spatial variability of the chemical composition of Late
489 Pleistocene loess-soil sequences of Poland in the context of palaeoenvironmental and palaeoclimatic changes"
490 (Principal Investigator: Jacek Skurzyński); and under the project No. 2017/27/B/ST10/01854 entitled "Sudden
491 COLD events of the Last Glacial in the central part of the European LOESS Belt – in Poland and in the western
492 part of Ukraine (COLD LOESS)" (Principal Investigator: Zdzisław Jary). We are grateful to editors (Nicholas
493 Lancaster and Randal Schaetzl) and two anonymous reviewers for their constructive comments and
494 suggestions.

495 496 **Appendix A. Supplementary data**

497 Supplementary data to this article can be found online at
498
499
500

501 REFERENCES

- 502 Andrews, J.T., Roth, W.J., Jennings, A.E., 2023. Grain size and mineral variability of glacial marine
503 sediments. *Journal of Sedimentary Research* 93, 37-49.
- 504 Badura, J., Jary, Z., Smalley, I., 2013. Sources of loess material for deposits in Poland and parts of Central
505 Europe: The lost big river. *Quaternary International* 296, 15-22.
- 506 Baykal, Y., Stevens, T., Engstrom-Johansson, A., Skurzyński, J., Zhang, H., He, J., Lu, H., Adamiec, G.,
507 Költringer, C., Jary, Z., 2021. Detrital zircon U-Pb age analysis of last glacial loess sources and
508 proglacial sediment dynamics in the Northern European Plain. *Quaternary Science Reviews* 274,
509 107265.
- 510 Bitelli, M., Andrenelli, M.C., Simonetti, G., Pellegrini, S., Artioli, G., Piccoli, I., Morari, F., 2019. Shall we
511 abandon sedimentation methods for particle size analysis in soils? *Soil and Tillage Research* 185, 36-
512 46.
- 513 Bosq, M., Bertran, P., Degeai, J-P., Queffelec, A., Moine, O., 2020. Geochemical signature of sources,
514 recycling and weathering in the Last Glacial loess from the Rhône Valley (southeast France) and
515 comparison with other European regions. *Aeolian Research* 42, 100561.
- 516 Bugge, B., Glaser, B., Hambach, U., Gerasimenko, N., Marković, S., 2011. An evaluation of geochemical
517 weathering indices in loess-paleosol studies. *Quaternary International* 240, 12-21.
- 518 Bugge, B., Glaser, B., Zoeller, L., Hambach, U., Marković, S., Glaser, I., Gerasimenko, N., 2008.
519 Geochemical characterization and origin of Southeastern and Eastern European loesses (Serbia,
520 Romania, Ukraine). *Quaternary Science Reviews* 27, 1058-1075.
- 521 Butrym, J., 1987. TL ages for loess profile in Odonów near Kazimierza Wielka. In: Madeyska, T. (Ed.),
522 *Scientific Research Report of Committee of Quaternary Research of the Polish Academy of Science* 7,
523 10-15.
- 524 Campodonico, V., Rouzaut, S., Pasquini, A., 2019. Geochemistry of a Late Quaternary loess-paleosol
525 sequence in central Argentina: Implications for weathering, sedimentary recycling and provenance.
526 *Geoderma* 351, 235-249.
- 527 Cegła, J., 1972. Sedymentacja lessów Polski. *Acta Universitatis Wratislaviensis* 168, 71 pp (in Polish).
- 528 Chayes, F., 1971. Ratio correlation. Chicago, *University of Chicago Press*, 99 p.

- 529 Condie, K.C., 1993. Chemical composition and evolution of the upper continental crust: contrasting results
530 from surface samples and shales. *Chemical Geology* 104, 1-37.
- 531 Derbyshire, E. 2001. Geological hazards in loess terrain, with particular reference to the loess regions of
532 China. *Earth Science Reviews* 54, 231-260.
- 533 Ebens, R.J., Connor, J.J., 1980. Geochemical survey of Missouri - Geochemistry of loess and carbonate
534 residuum. *U.S. Geological Survey Professional Paper*, 954-G.
- 535 Fenn, K., Millar, I.L., Durcan, J.A., Thomas, D.S.G., Banak, A., Marković, S.B., Veres, D., Stevens, T., 2022.
536 The provenance of Danubian loess. *Earth-Science Reviews* 226, 103920.
- 537 Fenn, K., Prud'Homme, C., 2022. Dust Deposits: Loess. In: Schroder, J.F., Lancaster, N. (Eds.), *Treatise on*
538 *Geomorphology*. Elsevier, pp. 320-365.
- 539 Fenn, K., Thomas, D.S.G., Durcan J.A., Millar, I.L., Veres, D., Piermattei, A., Lane, C.S., 2021. A tale of
540 two signals: Global and local influences on the Late Pleistocene loess sequences in Bulgarian Lower
541 Danube. *Quaternary Science Reviews* 274, 107264.
- 542 Finke, P., Hutson, J.L., 2008. Modelling soil genesis in calcareous löss. *Geoderma* 145 (3), 462-479.
- 543 Gallet, S., Jahn, B., Van Vliet Lanoe, B., Dia, A., Rossello, E., 1998. Loess geochemistry and its implications
544 for particle origin and composition of the upper continental crust. *Earth and Planetary Science Letters*
545 156, 157-172.
- 546 Guan, H., Zhu, C., Zhu, T., Wu, L., Li, Y., 2016. Grain size, magnetic susceptibility and geochemical
547 characteristics of the loess in the Chaohu lake basin: Implications for the origin, paleoclimatic change
548 and provenance. *Journal of Asian Earth Sciences* 117, 170-183.
- 549 Guo, Z., 2010. Loess geochemistry and Cenozoic paleoenvironments. *Geochemical news* 143, 1-10.
- 550 Han, L., Hao, Q., Qiao, Y., Wang, L., Peng, S., Li, N., Gao, X., Xu, B., Gu, Z., 2019. Geochemical evidence
551 for provenance diversity of loess in southern China and its implications for glacial aridification of the
552 northern subtropical region. *Quaternary Science Reviews* 212, 149-163.
- 553 Hao, Q., Guo, Z., Qiao, Y., Xu, B., Oldfield, F., 2010. Geochemical evidence for the provenance of middle
554 Pleistocene loess deposits in southern China. *Quaternary Science Reviews* 29, 3317-3326.
- 555 Jahn, A., 1950. Loess, its origin and connection with the climate of the glacial epoch. *Acta Geologica Polonica*
556 I(3), 257-310 (in Polish, with English Abstract).

- 557 Jahn, B., Gallet, S., Han, J., 2001. Geochemistry of the Xining, Xifeng and Jixian sections, Loess Plateau of
558 China: eolian dust provenance and paleosol evolution during the last 140 ka. *Chemical Geology* 178,
559 71-94.
- 560 Jary, Z., 2007. Record of Climate Changes in Upper Pleistocene loess-soil sequences in Poland and western
561 part of Ukraine. *Rozprawy Naukowe Instytutu Geografii i Rozwoju Regionalnego Uniwersytetu*
562 *Wrocławskiego* 1. Wrocław (in Polish, with English Abstract).
- 563 Jary, Z., Ciszek, D., 2013. Late Pleistocene loess-palaeosol sequences in Poland and western Ukraine.
564 *Quaternary International* 296, 37-50.
- 565 Jeong, G., Hillier, S., Kemp, R., 2008. Quantitative bulk and single-particle mineralogy of a thick Chinese
566 loess-paleosol section: implications for loess provenance and weathering. *Quaternary Science Reviews*
567 27, 1271-1287.
- 568 Jersak, J., 1973. Lithology and stratigraphy of the loess on the Southern Polish Uplands. *Acta Geographica*
569 *Lodziensia* 32, Łódź (in Polish, with English Abstract).
- 570 Kabata-Pendias, A., Pendias, H., 1999. Biogeochemia pierwiastków śladowych. *Wydawnictwo PWN*,
571 Warszawa, 398 pp (in Polish).
- 572 Kemp, R.A., 2001. Pedogenic modification of loess: significance for palaeoclimatic reconstructions. *Earth-*
573 *Science Reviews* 54, 145-156.
- 574 Költringer, C., Stevens, T., Lindner, M., Baykal, Y., Ghafarpour, A., Khormali, F., Taratunina, N., Kurbanov,
575 R., 2022. Quaternary sediment sources and loess transport pathways in the Black Sea - Caspian Sea
576 region identified by detrital zircon U-Pb geochronology. *Global and Planetary Change* 209, 103736.
- 577 Konert, M., Vandenberghe, J., 1997. Comparison of laser grain size analysis with pipette and sieve analysis:
578 a solution for the underestimation of the clay fraction. *Sedimentology* 44 (3), 523-535.
- 579 Krawczyk, M., Ryzner, K., Skurzyński, J., Jary, Z., 2017. Lithological indicators of loess sedimentation of
580 SW Poland. *Contemporary Trends in Geoscience* 6 (2), 94-111.
- 581 Kukla, G., An, S., 1989. Loess stratigraphy in central China. *Palaeogeography, Palaeoclimatology,*
582 *Palaeoecology* 72, 203-225.
- 583 Lehmkühl, F., Nett, J.J., Potter, S., Schulte, P., Sprafke, T., Jary, Z., Antoine, P., Wacha, L., Wolf, D., Zerboni,
584 A., Hosek, J., Marković, S.B., Obreht, I., Sumegi, P., Veres, D., Zeeden, C., Boemke, B., Schaubert,

585 V., Viehweger, J., Hambach, U., 2021. Loess landscapes of Europe – Mapping, geomorphology, and
586 zonal differentiation. *Earth-Science Reviews* 215, 103496.

587 Lehmkuhl, F., Zens, J., Krauß, L., Schulte, P., Kels, H., 2016. Loess-paleosol sequences at the northern
588 European loess belt in Germany: Distribution, geomorphology and stratigraphy. *Quaternary Science
589 Reviews* 153 (1), 11-30.

590 Li, Z., Chen, Q., Dong, S., Zhang, D., Yu, X., Zhang, C., 2021. Applicability of rare earth elements in eolian
591 sands from desert as proxies for provenance: A case study in the Badain Jaran Desert, Northwestern
592 China. *Catena* 207, 105647.

593 Licht, A., Pullen, A., Kapp, P., Abell, J., Giesler, N., 2016. Eolian cannibalism: Reworked loess and fluvial
594 sediment as the main sources of the Chinese Loess Plateau. *GSA Bulletin* 128 (5-6), 944-956.

595 Lis, J., Pasieczna, A., 2006. Geochemical characteristics of soil and stream sediment in the area of glacial
596 deposits in Europe. In: Tarvainen, T., De Vos, W. (Eds.), *Geochemical Atlas of Europe. Part 2.
597 Interpretation of Geochemical Maps, Additional Tables, Figures, Maps, and Related Publications.*
598 Geological Survey of Finland, Espoo, pp. 519–540.

599 Liu, T.S., 1985. *Loess and the Environment*. China Ocean Press, Beijing, 251 pp.

600 Lukashev, K.I., Lukashev, V.K., Dobroval'skaya, I.A., 1965. Litho-geochemical properties of loess in
601 Byelorussia and Central Asia. [In:] Schultz, C.B., Freye, C., *Loess and related eolian deposits of the
602 world*. Inqua Loess Conference, USA.

603 Marković, S., Bokhorst, M., Vanderberghe, J., McCoy, W., Oches, E., Hambach, U., 2008. Late Pleistocene
604 loess-paleosol sequences in the Vojvodina region, north Serbia. *Journal of Quaternary Science* 23, 73-
605 84.

606 Marković, S., Stevens, T., Kukla, G.J., Hambach, U., Fitzsimmons, K.E., Gibbard, P., Buggle, B., Zech, M.,
607 Guo, Z., Hao, Q., Wu, H., Ken O'Hara, D., Smalley, J., Újvári, G., Sümegi, P., Timar-Gabor, A.,
608 Veres, D., Sirocko, F., Vasilijević, A., Jary, Z., Svensson, A., Jović, V., Lehmkuhl, F., Kovacs, J.,
609 Svircev, Z. 2015. Danube loess stratigraphy - Towards a pan-European loess stratigraphic model.
610 *Quaternary Science Reviews* 148, 228-258.

611 Maruszczak, H., 1991. Stratigraphical differentiation of Polish loesses. In: Maruszczak, H. (Ed.), *Main
612 sections of loesses in Poland*, UMCS, Lublin, 13-35 (in Polish, with English Abstract).

- 613 McLennan, S.M., 1993. Weathering and global denudation. *Journal of Geology* 101, 295-303.
- 614 McLennan, S.M., 2001. Relationships between the trace element composition of sedimentary rocks and upper
615 continental crust. *Geochemistry, Geophysics, Geosystems* 2 (4).
- 616 Miller, B.A., Schaetzl, R.J., 2012. Precision of Soil Particle Size Analysis using Laser Diffractometry. *Soil
617 Science Society of America Journal* 76 (5), 1719-1727.
- 618 Miyazaki, T., Kimura, J.I., Katakuse, M., 2016. Geochemical records from loess deposits in Japan over the
619 last 210 kyr: lithogenic source changes and paleoclimatic indications. *Geochemistry, Geophysics,
620 Geosystems* 17, 2745-2761.
- 621 Moska, P., Adamiec, G., Jary, Z., Bluszcz, A., 2017. OSL chronostratigraphy for loess deposits from
622 Tyszowce – Poland. *Geochronometria* 44/1, 307-318.
- 623 Moska, P., Adamiec, G., Jary, Z., Bluszcz, A., Poręba, G., Piotrowska, N., Krawczyk, M., Skurzyński, J.,
624 2018. Luminescence chronostratigraphy for the loess deposits in Złota, Poland. *Geochronometria* 45,
625 44-55.
- 626 Moska, P., Bluszcz, A., 2013. Luminescence dating of loess profiles in Poland. *Quaternary International* 296,
627 51-60.
- 628 Moska, P., Jary, Z., Adamiec, G., Bluszcz, A., 2019a. Chronostratigraphy of a loess-palaeosol sequence in
629 Biały Kościół, Poland using OSL and radiocarbon dating. *Quaternary International* 502, 4-17.
- 630 Moska, P., Jary, Z., Adamiec, G., Bluszcz, A., 2019b. High resolution dating of loess profile from Strzyżów
631 (Horodło Plateau-Ridge, Volhynia Upland). *Quaternary International* 502, 18-29.
- 632 Mroczek, P., 2013. Recycled loesses – a micromorphological approach to the determination of local source
633 areas of Weichselian loess. *Quaternary International* 296, 241-250.
- 634 Muhs, D.R., 2018. The geochemistry of loess: Asian and North American deposits compared. *Journal of Asian
635 Earth Sciences* 155, 81-115.
- 636 Muhs, D.R., Bettis, E.A., 2000. Geochemical variations in Peoria loess of Western Iowa indicate paleowinds
637 of midcontinental North America during last glaciation. *Quaternary Research* 53, 49-61.
- 638 Muhs, D.R., Budahn, J.R., 2006. Geochemical evidence for the origin of late Quaternary loess in central
639 Alaska. *Canadian Journal of Earth Sciences* 43, 323-337.

- 640 Nesbitt, H.W., 1979. Mobility and fractionation of rare earth elements during weathering of a granodiorite.
641 *Nature* 279, 206-210.
- 642 Nesbitt, H.W., Young, G.M., 1982. Early proterozoic climate and plate motions inferred from major element
643 chemistry of lutites. *Nature* 229, 715-717.
- 644 Nesbitt, H.W., Young, G.M., 1984. Prediction of some weathering trends of plutonic and volcanic rocks based
645 on thermodynamic and kinetic considerations. *Geochimica et Cosmochimica Acta* 48, 1523-1534.
- 646 Nesbitt, H.W., Young, G.M., McLennan, M., Keays, R.R., 1996. Effects of Chemical Weathering and Sorting
647 on the Petrogenesis of Siliciclastic Sediments, with Implications for Provenance Studies. *The Journal*
648 *of Geology* 104 (5), 525-542.
- 649 Obreht, I., Zeeden, C., Schulte, P., Hambach, U., Eckmeier, E., Timar-Gabor, A., Lehmkuhl, F., 2015. Aeolian
650 dynamics at the Orlovat loess–paleosol sequence, northern Serbia, based on detailed textural and
651 geochemical evidence. *Aeolian Research* 18, 69-81.
- 652 Pańczyk M., Nawrocki J., Bogucki A.B., Gozhik P., Łanczont M., 2020. Possible sources and transport
653 pathways of loess deposited in Poland and Ukraine from detrital zircon U-Pb age spectra. *Aeolian*
654 *Research* 45, 100598.
- 655 Pötter, S., Seeger, K., Richter, C., Brill, D., Knaak, M., Lehmkuhl, F., and Schulte, P., 2023. Pleniglacial
656 dynamics in an oceanic central European loess landscape. *E&G Quaternary Science Journal* 72, 77-
657 94.
- 658 Pötter, S., Veres, D., Baykal, Y., Nett, J.J., Schulte, P., Hambach, U., Lehmkuhl, F., 2021. Disentangling
659 Sedimentary Pathways for the Pleniglacial Lower Danube Loess Based on Geochemical Signatures.
660 *Frontiers in Earth Science* 9, 600010.
- 661 Pye, K., 1984. Loess. *Progress in Physical Geography* 8, 176-217.
- 662 Reeder, S., Taylor, H., Shaw, R.A., Demetriades, A., 2006. Introduction to the chemistry and geochemistry of
663 the elements. In: Tarvainen T., De Vos W. (Eds.), *Geochemical Atlas of Europe. Part 2. Interpretation*
664 *of Geochemical Maps, Additional Tables, Figures, Maps, and Related Publications*. Geological Survey
665 of Finland, Espoo, pp. 48–429.
- 666 Rock, N.M.S., 1987. The need for standardization of normalised multi-elemental diagrams in geochemistry:
667 a comment. *Geochemical Journal* 21, 75-84.

668 Rollinson, H., 2013. Using geochemical data: evaluation, presentation, interpretation. Routledge.

669 Rousseau, D.-D., Chauvel, C., Sima, A., Hatte, C., Lagroix, F., Antoine, P., Balkanski, Y., Fuchs, M., Mellett,
670 C., Kageyama, M., Ramstein, G., Lang, A., 2014. European glacial dust deposits: Geochemical
671 constraints on atmospheric dust cycle modeling. *Geophysical Research Letters* 41, 7666-7674.

672 Rousseau, D.-D., Derbyshire, E., Antoine, P., Hatté C., 2018. European Loess Records. *Reference Module in*
673 *Earth Systems and Environmental Sciences*, Elsevier.

674 Rudnick, R.L., Gao, S., 2003. Composition of the continental crust. In: Holland, H.D., Turekian, K.K. (Eds.),
675 *Treatise on Geochemistry*, vol. 3. Elsevier-Pergamon, Oxford-London, pp. 1-64.

676 Schaetzl, R.J., Attig, J.W., 2013. The loess cover of northeastern Wisconsin. *Quaternary Research* 79, 199-
677 214.

678 Schaetzl, R.J., Bettis III, A., Crouvi, O., Fitzsimmons, K.E., Grimley, D.A., Hambach, U., Lehmkuhl, F.,
679 Marković, S.B., Mason, J.A., Owczarek, P., Roberts, H.M., Rousseau, D.-D., Stevens, T.,
680 Vandenberghe, J., Zárate, M., Veres, D., Yang, S., Zech, M., Conroy, J.L., Dave, A.K., Faust, D., Hao,
681 Q., Obreht, I., Prud'homme, C., Smalley, I., Tripaldi, A., Zeeden, C., Zech, R., 2018. Approaches and
682 challenges to the study of loess - Introduction to the LoessFest Special Issue. *Quaternary Research* 89
683 (3), 563-618.

684 Scheib, A.J., Birke, M., Dinelli, E., GEMAS Project Team, 2014. Geochemical evidence of aeolian deposits
685 in European soils: geochemical evidence of aeolian deposits in European soils. *Boreas* 43, 175-192.

686 Schnetger, B., 1992. Chemical composition of loess from a local and worldwide view. *Neues Jahrbuch für*
687 *Mineralogie Monatshefte* 1, 29-47.

688 Shao, J., Yang, S., Li, C., 2012. Chemical indices (CIA and WIP) as proxies for integrated chemical
689 weathering in China: inferences from analysis of fluvial sediments. *Sedimentary Geology* 265-266,
690 110-120.

691 Sheldon, N.D., Tabor, N.J., 2009. Quantitative paleoenvironmental and paleoclimatic reconstruction using
692 paleosols. *Earth-Science Reviews* 95, 1-52.

693 Shepard, F.P., 1954. Nomenclature Based on Sand-silt-clay Ratios. *Journal of Sedimentary Research* 24 (3),
694 151-158.

- 695 Shi, Y., E, C., Peng, Q., Zhang, Z., Zhang, J., Yan, W., Xu, C., 2023. Rare earth elements in aeolian loess
696 sediments from Menyuan Basin, northeastern Tibetan plateau: Implications for provenance. *Frontiers*
697 *in Environmental Science* 11, 1074909.
- 698 Sial, A.N., Gaucher, C., Ramkumar, M., Ferreira, V.P., 2019. Chemostratigraphy as a Formal Stratigraphic
699 Method In: Sial A.N., Gaucher C., Ramkumar M., Ferreira V.P., *Chemostratigraphy Across Major*
700 *Chronological Boundaries*, Geophysical Monograph, 240. John Wiley & Sons.
- 701 Skurzyński, J., Fenn, K., 2022. Wpływ aspektów metodycznych na poprawność paleośrodowiskowych
702 interpretacji zmienności cech geochemicznych w lessach. In: Łanczont, M., Hołub, M., Mroczek, P.
703 (Eds.), *Metodyka rekonstrukcji zmian klimatu i środowiska zapisanych w pokrywach lessowych. XXI*
704 *Terenowe Seminarium Korelacja lessów i osadów glacialnych Polski i Ukrainy. Interdyscyplinarne*
705 *Seminarium Naukowe Glacjał i peryglacjał Europy Środkowej*. Jarosław, 6-8 października 2022 r.,
706 Lublin (in Polish).
- 707 Skurzyński, J., Jary, Z., Kenis, P., Kubik, R., Moska, P., Raczyk, J., Seul, C., 2020. Geochemistry and
708 mineralogy of the Late Pleistocene loess-palaeosol sequence in Złota (near Sandomierz, Poland):
709 Implications for weathering, sedimentary recycling and provenance. *Geoderma* 375, 114459.
- 710 Skurzyński, J., Jary, Z., Raczyk, J., Moska, P., Korabiewski, B., Ryzner, K., Krawczyk, M., 2019.
711 Geochemical characterization of the Late Pleistocene loess-palaeosol sequence in Tyszowce (Sokal
712 Plateau-Ridge, SE Poland). *Quaternary International* 502, 108-118.
- 713 Skurzyński, J., Modelska, M., Raczyk, J., Staśko, S., Jary, Z., 2017. Skład chemiczny wód porowych
714 górnoplejstoczeńskiej sekwencji lessowo-glebowej w Zaprężynie (SW Polska). *Przegląd Geologiczny*
715 65 (11/2), 1383-1387 (in Polish, with English Abstract).
- 716 Smalley, I., Vita-Finzi, C., 1968. The formation of fine particles in sandy deserts and the nature of „desert”
717 loess. *Journal of Sedimentary Research* 38 (3), 766-774.
- 718 Smalley, I.J., Leach, J.A., 1978. The origin and distribution of the loess in the Danube basin and associated
719 regions of East-Central Europe: a review. *Sedimentary Geology* 21, 1-26.
- 720 Smalley, I.J., O’Hara-Dhand, K., Wint, J., Machalett, B., Jary, Z., Jefferson, I.F., 2009. Rivers and loess: the
721 significance of long river transportation in the complex event-sequence approach to loess deposit
722 formation. *Quaternary International* 198, 7-18.

723 Song, Y., Chen, X., Qian, L., Li, C., Li, Y., Li, X., 2014. Distribution and composition of loess sediments in
724 the Ili Basin, Central Asia. *Quaternary International* 334-335, 61-73.

725 Stevens, T., Adamiec, G., Bird, A.F., Lu, H., 2013. An abrupt shift in dust source on the Chinese Loess Plateau
726 revealed through high sampling resolution OSL dating. *Quaternary Science Reviews* 82, 121-132.

727 Svensson, D.N., Messing, I., Barron, J., 2022. An investigation in laser diffraction soil particle size distribution
728 analysis to obtain compatible results with sieve and pipette method. *Soil and Tillage Research* 223,
729 105450.

730 Taylor, S.R., McLennan, S.M., 1985. The Continental Crust: Its Composition and Evolution. Blackwell,
731 London.

732 Taylor, S.R., McLennan, S.M., McCulloch, M.T., 1983. Geochemistry of loess, continental crustal
733 composition and crustal model ages. *Geochimica et Cosmochimica Acta* 47, 1987-1905.

734 Templ, M., Filzmoser, P., Reimann, C., 2008. Cluster analysis applied to regional geochemical data: problems
735 and possibilities. *Applied Geochemistry* 23, 2198-2213.

736 Tripathi, J.K., Rajamani, V., 1999. Geochemistry of the loessic sediments on Delhi ridge, eastern Thar desert,
737 Rajasthan: implications for exogenic processes. *Chemical Geology* 155, 265-278.

738 Tu, X.B., Kwong, A.K.L., Dai, F.C., Tham, L.G., Min, H. 2009. Field monitoring of rainfall infiltration in a
739 loess slope and analysis of failure mechanism of rainfall-induced landslides. *Engineering Geology* 105,
740 134–150.

741 Tutkovsky, P.A., 1899. K voprosu o sposobe obrazovaniya lessa. *Zemlevedenie* 1-2, 213-311 (in Russian).

742 Újvári, G., Varga, A., Raucsik, B., Kovacs, J., 2014. The Paks loess-paleosol sequence: A record of chemical
743 weathering and provenance for the last 800 ka in the mid-Carpathian Basin. *Quaternary International*
744 319, 22-37.

745 Újvári, G., Varga, A., Balogh-Brunstad, Z., 2008. Origin, weathering, and geochemical composition of loess
746 in southwestern Hungary. *Quaternary Research* 69, 421-437.

747 Van Loon, A.J., 2006. Lost loesses. *Earth-Science Reviews* 74 (3-4), 309-316.

748 Varga, A., Újvári, G., Raucsik, B., 2011. Tectonic versus climatic control on the evolution of a loess-paleosol
749 sequence at Beremend, Hungary: An integrated approach based on paleoecological, clay
750 mineralogical, and geochemical data. *Quaternary International* 240, 71-86.

751 Waroszewski, J., Pietranik, A., Sprafke, T., Kabała, C., Frechen, M., Jary, Z., Kot, A., Tsukamoto, S., Meyer-
752 Heintze, S., Krawczyk, M., Łabaz, B., Schultz, B., Erban Kochergina, Y.V., 2021. Provenance and
753 paleoenvironmental context of the Late Pleistocene thin aeolian silt mantles in southwestern Poland –
754 A widespread parent material for soils. *Catena* 204, 105377.

755 Wentworth, C.K., 1922. A scale of grade and class terms for clastic-sediments. *The Journal of Geology* 30
756 (5), 377-392.

757 Wilson, M. J., 2004. Weathering of the primary rock-forming minerals: processes, products and rates. *Clay*
758 *Minerals* 39, 233-266.

759 Wright, J.S., Smith, B., Whalley, B., 1998. Mechanisms of loess-sized quartz silt production and their relative
760 effectiveness: laboratory simulations. *Geomorphology* 23, 15-34.

761 Yang, S., Ding, F., Ding, Z., 2006. Pleistocene chemical weathering history of Asian arid and semi-arid
762 regions recorded in loess deposits of China and Tajikistan. *Geochimica et Cosmochimica Acta* 70,
763 1695-1709.

764 Zeng, R.Q., Meng, X.M., Zhang, F.Y., Wang, S.Y., Cui, Z.J., Zhang, M.S., Zhang, Y., Chen, G. 2016.
765 Characterizing hydrological processes on loess slopes using electrical resistivity tomography – A case
766 study of the Heifangtai Terrace, Northwest China. *Journal of Hydrology* 541,742-753.

767 Zöller, L., Fischer, M., Jary, Z., Antoine, P., Krawczyk, M., 2022. Chronostratigraphic and geomorphologic
768 challenges of last glacial loess in Poland in the light of new luminescence ages. *E&G Quaternary*
769 *Science Journal* 71, 59-81.

770

771 **Figures:**

772 Fig. 1. Location of the research sites on a map of loess distribution in Poland (A) and Europe (B) (loess
773 distribution after Lehmkuhl et al, 2021).

774 Fig. 2. Schemes of the main research sites. Abbreviations: STR – stratigraphy, L + S – lithology + samples,
775 A – ages (expressed as ka). Stratigraphical labelling system after Kukla and An (1989), modified by
776 Marković et al. (2008, 2015): S0 – recent soil, L1LL1 – loess correlated to MIS 2, L1SS1 – paleosol
777 correlated to MIS 3, L1LL2 – loess correlated to MIS 4, S1 – paleosol complex correlated to MIS 5.
778 U.M.* means “underlying material”. Lithological legend: dark grey rectangles – soil units; pale grey

779 rectangles – horizons with signs of gley processes or deformations; pale grey rectangle with black
780 curves – loess with gley and humic intercalations. Black spots – geochemical samples. Ages after
781 Moska et al. (2017, 2018, 2019a) – Post-IR IRSL polymineral fraction (4–11 μm).

782 Fig. 3. The variability of the main elements (100 wt.% without the volatile components) at the research sites.
783 Vertical grey dashed lines represent GAL values (Újvári et al., 2008) for individual oxides. The main
784 pedo- and lithostratigraphic units are also drawn. Legend of lithological markings according to Fig. 2.

785 Fig. 4. The variability of the trace elements (ppm) at the research sites. The main pedo- and lithostratigraphic
786 units are also drawn. Legend of lithological markings according to Fig. 2.

787 Fig. 5. The variability of the rare earth elements (ppm) at the research sites. The main pedo- and
788 lithostratigraphic units are also drawn. Legend of lithological markings according to Fig. 2.

789 Fig. 6. A-CN-K ternary diagram (Nesbitt and Young, 1984) of the Polish loess samples. CaO^* (Ca in silicates)
790 was calculated according to McLennan (1993). Dashed lines – CIA values of 65 and 85. Stratigraphical
791 labelling system after Kukla and An (1989), modified by Marković et al. (2008, 2015).

792 Fig. 7. UCC-normalized multielemental spidergrams for Polish loess. Each curve represents one sample. Ni
793 is not shown because of its presence only in some samples. The UCC values used are from Rudnick
794 and Gao (2003).

795 Fig. 8. Th/Sc vs Zr/Sc discrimination diagram of sedimentary recycling (McLennan et al., 1993) for Polish
796 loess. Explanations: A – BK 3.8 - 5.3; ZŁ 6.05 - 6.9; TY 10.45 - 11.35, 12.95 and 13.9 - 14.6; OD 2.5
797 m. B – BK 1.36 - 3.6 (except 2.06 and 2.25); ZŁ 2.6 and 5.25; OD 3.3 m. C – BK 2.06 and 2.25; ZŁ
798 1.75 and 4.65; TY 6 - 6.65 m, 8.8, 9.55 - 10, 12.25 - 12.55, 13.35; ST - 5; ZA - 1.2 m, D – ZŁ 0.55 -
799 1.4, 2.2, 3.3 - 4, 5.05, 5.45 - 5.6; OD 0.9 - 1.8; ST 3.2 - 3.8; ZA - 1.5 m. E – TY 1 - 5.35, 7.15 8.15,
800 9.1, 11.75 - 11.95; ST 4.4, 7.3 - 9.3; ZA - 1.65 m. Zoomed area is not in the scale.

801 Fig. 9. Box plots of Gd_N/Yb_N values of Polish and European loess. Explanations: signature of red square -
802 median, whiskers - range of values, frame - 25-75% of values. Explanations for the data from literature
803 (colored polygons): – red rectangle (the data from Bosq et al., 2020) shows the samples from Rhine
804 (Achenheim, Nussloch) and Rhône (Baix, Bouzil, Brillanne, Collias, Cuges les Pins, Donnat,
805 Lautagne, Mauves, Pact, Serezin du Rhône, Saint Julien de Peyrolas, Saint Paul les Durance, Vaise);
806 yellow rectangle (the data from Bosq et al., 2020) shows the samples form N France (Quesnoy,

Hauteville), Germany - Saxony (Rottewitz), Rhine (Schaffhouse), Serbia (Surduk), Rhône (Feyzin, Garons, Lautagne, Ledenon, Montanay, Saint-Péray, Sathonay, Saint Cyr au Mont d'Or, Saint-Désirat, Saint Georges les Bains, Soyons, Tain l'Hermitage); green rectangle (the data from Bosq et al., 2020) shows the samples from N France (Beutin, Glos, Nisy le Comte, Sourdon, Verlinghem, Chaudon, Havrincourt, Renancourt, Villers Carbonnel), Aquitaine (Pomarez, Romentères), Belgium (Harmignies), Ukraine (Korshiv), E Germany (Ostrau), Poland (Tyszowce, Złota); blue rectangle (the data from Rousseau et al., 2014) shows the samples from W Germany (Nussloch; samples from following depths: 5, 6, 7.9, 9.5, 10.3, 12, 14.1, 17.8 m), W Europe (Pleneuf Val Andre, Languvoisin, Serbia (Surduk); grey rectangle (the data from Rousseau et al., 2014) shows the samples from W Europe (English Channel, Villers Carbonel, Harmignies), E Germany (Gleina, Leippen, Ostrau, Seilitz, Zehren, Zeuchfeld), Ukraine (Stayky).

Fig. 10. UCC-normalized and PML-normalized multielemental spidergrams for loess samples from Korshiv (Ukraine) and Surduk (Serbia) – geochemical data used for normalization after Bosq et al. (2020). Each curve represents one sample. Ni is not shown because of its presence only in some samples. The UCC values used are from Rudnick and Gao (2003), PML – this study.

Table 1. Polish Median Loess (PML – this study) versus UCC (Rudnick and Gao, 2003), AVL¹ (Schnetger, 1992; Újvári et al., 2008 - the AVL¹ presented by Újvári et al., 2008, lacks the values for Co, Cs, Hf, Ta, U, W, Pr, Nd, Sm, Eu, Gd, Tb, Dy, Ho, Er, Tm, Yb, and Lu, so these elements are cited after original "average loess" presented by Schnetger, 1992) and GAL (Újvári et al., 2008). Major elements (wt.%) are recalculated on a volatile-free basis. Total iron is expressed as Fe₂O₃ (Fe₂O₃ value of AVL¹ in this study was recalculated from FeO_(tot) = 2.78% as presented by Újvári et al. (2008). Schnetger (1992) presented separately FeO = 0.8%, and Fe₂O₃ = 2.2%). Trace elements and REE are in ppm. The color scale was developed using the Conditional Formatting function of MS Excel - the red-yellow-green color scale indicates the position of a given value in the entire range of values in a given column (red = high values, green = low values). N/D means “no data”.

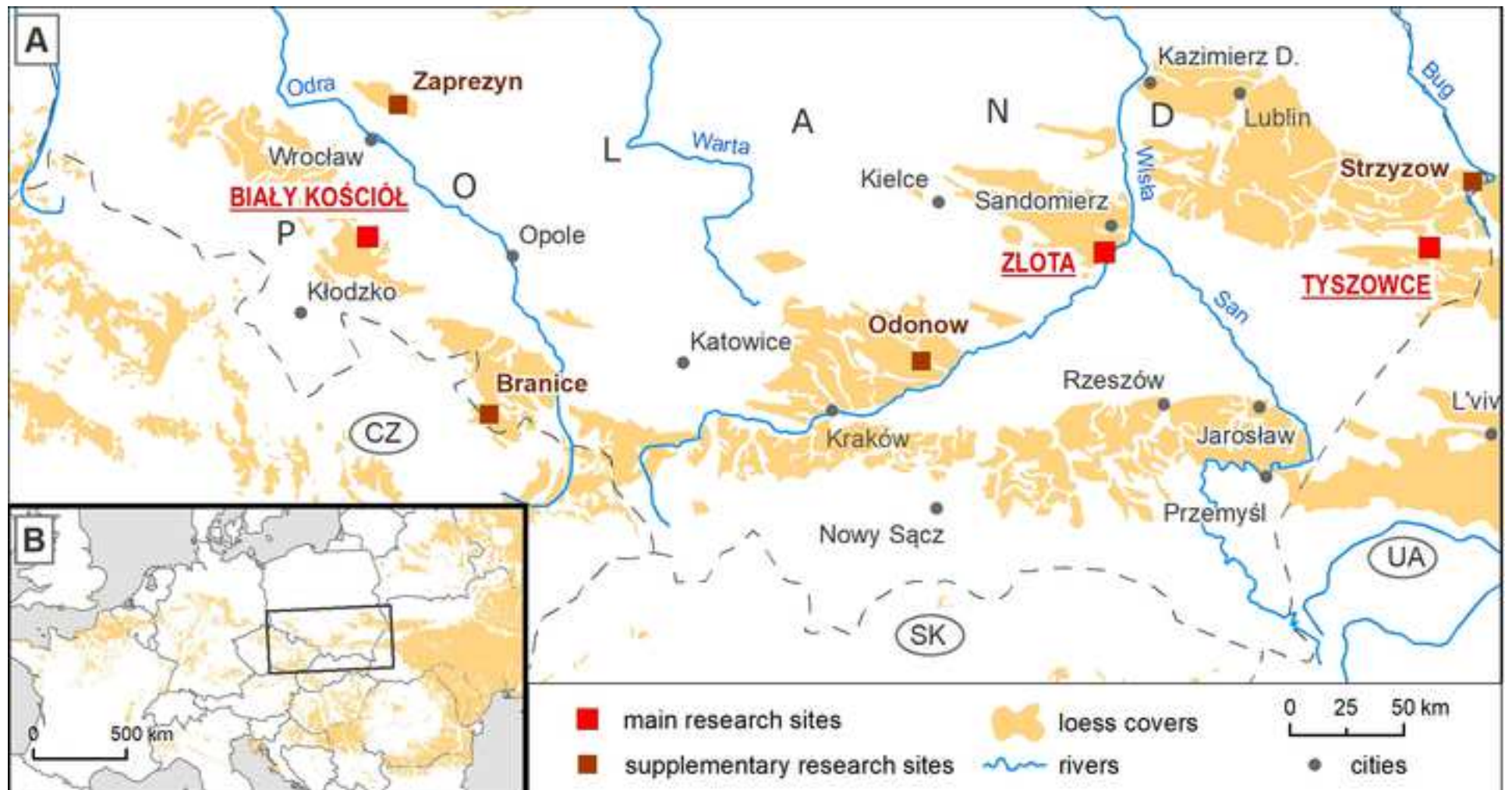
Dear Editors,

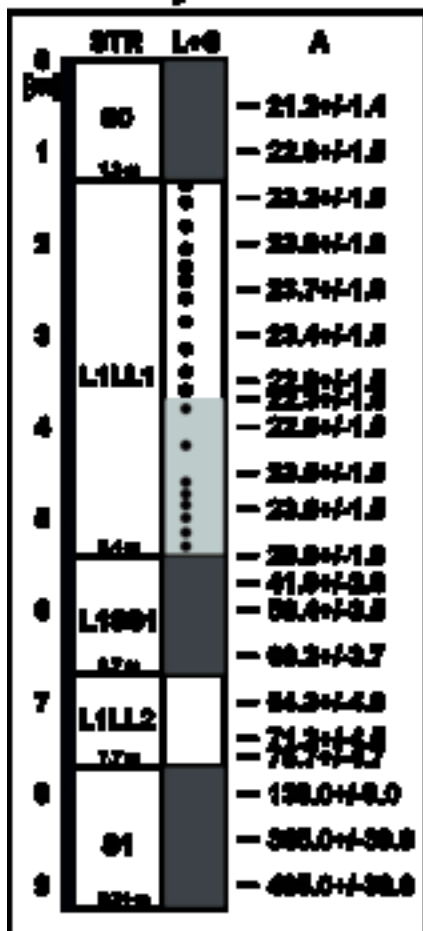
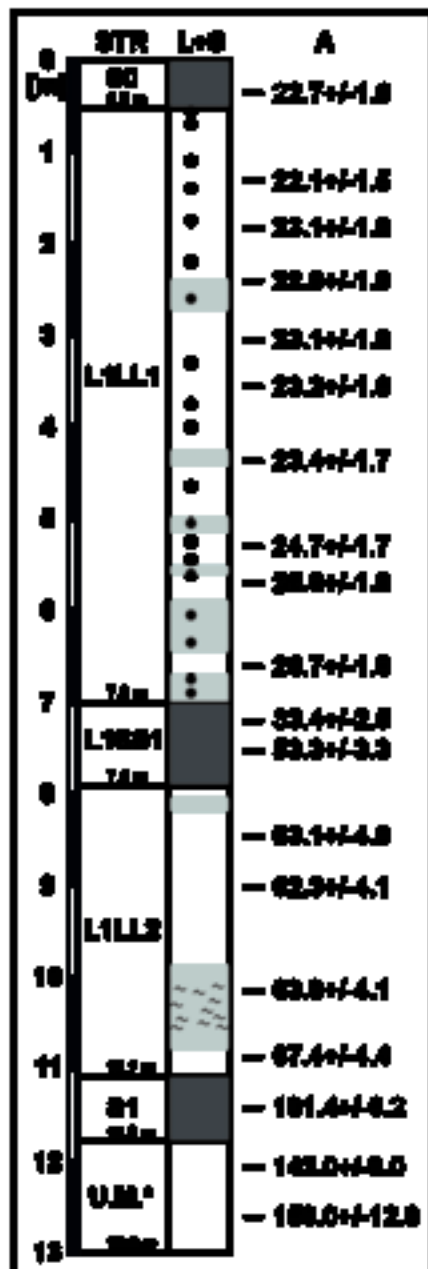
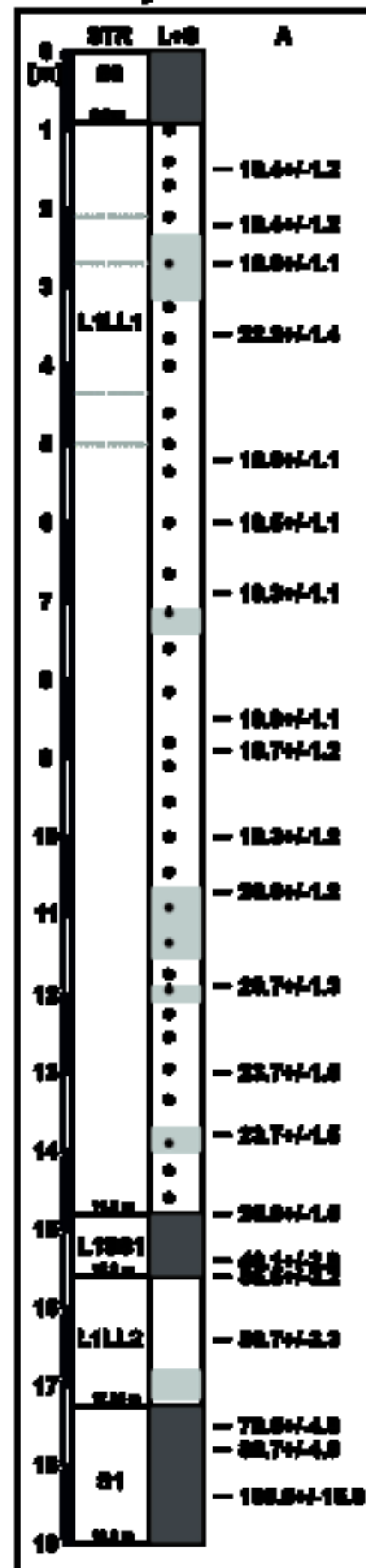
thank you for your really kind words and constructive comments. We have not mentioned most of the Editor's comments in this document - they have been unquestionably accepted. Comments that required clarification are presented below.

1. RS proposition: "At the same time, it is considered to be relatively homogeneous in terms of geochemical composition (Gallet et al., 1998; Wright, 1998; Tripathi and Rajamani, 1999; Újvári et al., 2008; Muhs, 2018; Fenn et al., 2022) due to its considerable spread and mixing during **aeolian** transport". It is not only aeolian, as shown later [lines 121-125]: "The loess cover of Poland relates to the very dynamic environment of Pleistocene glaciations (e.g., Tutkovsky, 1899; Jahn, 1950; Rousseau et al., 2014; Skurzyński et al., 2020) and was most likely sourced from glacial deposits, as homogenized by meltwater rivers (Smalley et al., 2009, Badura et al., 2013; Pańczyk et al., 2020; Baykal et al., 2021), with a variable proportion of local material (Pańczyk et al., 2020, Baykal et al., 2021)".
2. RS proposition: "**Three** supplementary sites, i.e. Zaprężyn (Jary, 2007; Krawczyk et al., 2017; Skurzyński et al., 2017; Zöller et al., 2022), Strzyżów (Moska et al., 2019b), Branice (Jary, 2007; Moska and Bluszcz, 2013) and Odonów (Butrym, 1987; Jary, 2007) were also investigated to determine the spatial variability of the chemical composition in the context of hetero- or homogeneity of the source material". We have four supplementary sites, not three...
3. RS proposition: "**Move this paragraph down, to the Methods section?** → In this work 70 L1LL1 (MIS 2) samples were subject to geochemical analysis (Biały Kościół – 19, Tyszowce – 32, Zaprężyn – 3, Strzyżów – 6, Odonów – 5, Branice – 5) following the methodology used previously for Złota loess-palaeosol sequence (Skurzyński et al., 2020). A further 19 published samples for Złota's (Skurzyński et al., 2020) L1LL1 loess were also included, resulting in a total of 89 L1LL1 (MIS 2) loess samples under study." It is placed in the chapter "research area and materials". We believe that it is OK.
4. "The share of medium dust (**RS proposition loess → I believe that we only call it dust when it is in the air; otherwise it is loess**) (16-31 μm) is comparable to other supplementary sites (Table S2, Table S3). Of course we thought silt, as a granulometric fraction... It is modified.
5. RS comment: "Suggest citing a paper here, which uses this value and which also justifies its use. Other clay-silt boundaries have been used by other researchers, so please justify this". Original phrase: "The clay-silt boundary assigned to the samples was 4 μm ". Modified phrase: "The clay-silt boundary assigned to the samples was 4 μm (e.g., Svensson et al., 2022), so the clay fraction may be underestimated in relation to the data from publications utilizing higher clay-silt boundary, e.g. 8 μm (Konert and Vandenberghe, 1997)".
6. RS comment: "Do you want to mention which one? And what the implications of this might be?". Original phrase: "The Kruskal-Wallis test (Table S4), in which the null hypothesis is that the medians of each group are the same, showed that at least one main research site the loess chemical composition differs significantly from the others, by the median of practically each of the determined chemical elements (except MgO, P₂O₅, MnO, Ni, and Zr)". The entire rest of this chapter is actually a response to this comment, so we left it as it is.
7. RS comment: "I like this - good justification". Authors response: thank you! 😊

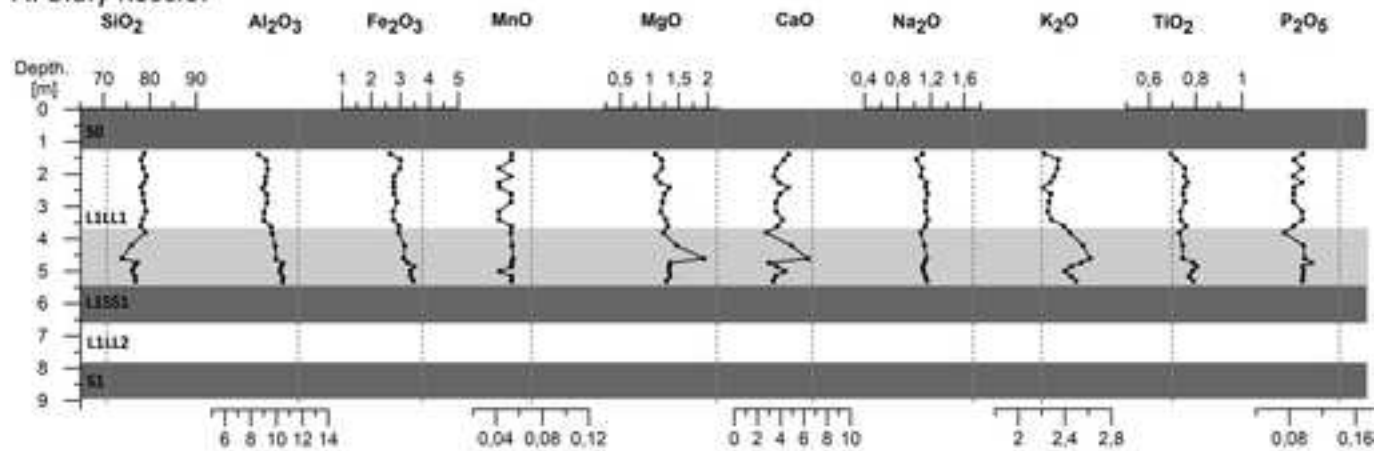
Table 1

	PML	UCC	AVL ^{1*}	GAL
SiO ₂	78.64	66.00	76.50	70.71
Al ₂ O ₃	8.19	15.20	12.50	11.74
Fe ₂ O ₃	2.41	5.00	3.09	3.75
MgO	1.32	2.20	1.00	2.15
CaO	4.81	4.20	1.30	6.67
Na ₂ O	1.07	3.90	2.10	1.68
K ₂ O	2.25	3.40	2.30	2.22
TiO ₂	0.68	0.50	0.63	0.71
P ₂ O ₅	0.10	0.40	N/D	0.14
MnO	0.04	0.08	0.06	0.07
Cr	68.42	62.00	43.00	67.00
Ba	360.00	628.00	582.00	427.00
Ni	22.00	47.00	18.00	27.00
Sc	6.00	14.00	8.00	N/D
Co	5.50	17.30	9.00	N/D
Cs	2.40	4.90	3.70	N/D
Ga	7.90	17.50	13.00	12.00
Hf	14.60	5.30	12.00	N/D
Nb	12.80	12.00	18.00	14.00
Rb	69.20	84.00	81.00	79.00
Sr	131.10	320.00	246.00	208.00
Ta	0.90	0.90	1.30	N/D
Th	9.50	10.50	10.00	9.00
U	2.70	2.70	2.60	N/D
V	46.00	97.00	66.00	N/D
W	1.4	1.90	1.30	N/D
Zr	576.2	193.00	387.00	322
Y	27.8	21.00	25.00	26
La	30.8	31.00	35.00	29
Ce	59.8	63.00	78.00	61
Pr	6.86	7.10	8.40	N/D
Nd	26.3	27.00	33.00	N/D
Sm	5.01	4.70	6.40	N/D
Eu	0.88	1.00	1.20	N/D
Gd	4.69	4.00	4.80	N/D
Tb	0.75	0.70	0.80	N/D
Dy	4.68	3.90	4.70	N/D
Ho	0.99	0.83	1.00	N/D
Er	3.06	2.30	2.80	N/D
Tm	0.45	0.30	N/D	N/D
Yb	3.08	1.96	2.70	N/D
Lu	0.48	0.31	N/D	N/D

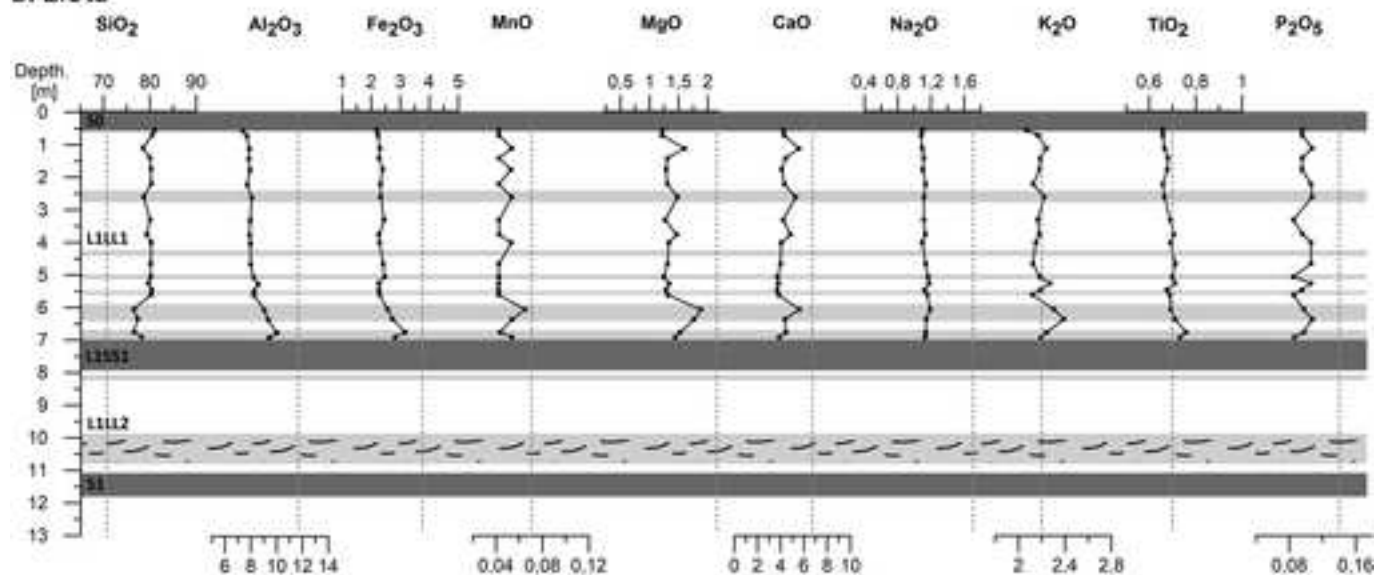


Biały Kościół**Złota****Tyszowce**

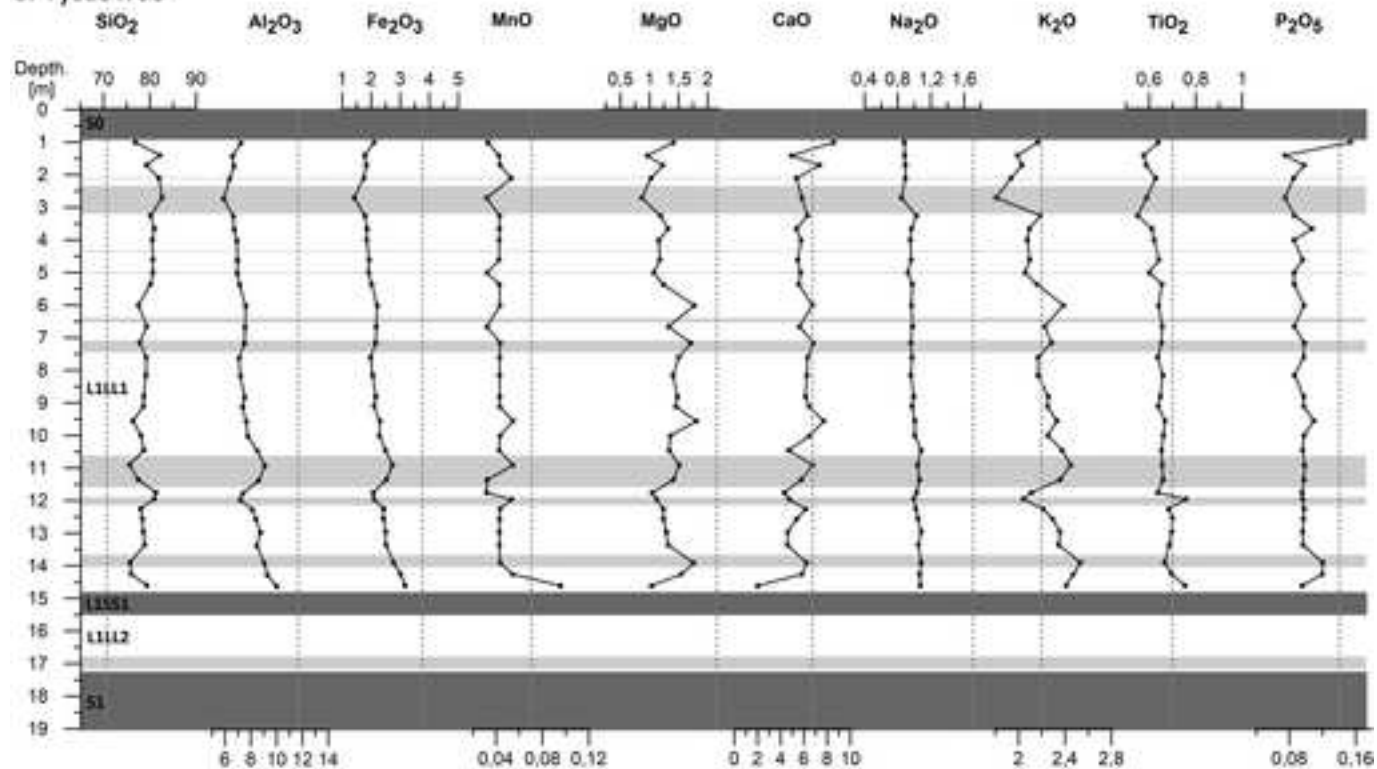
A. Biały Kościół



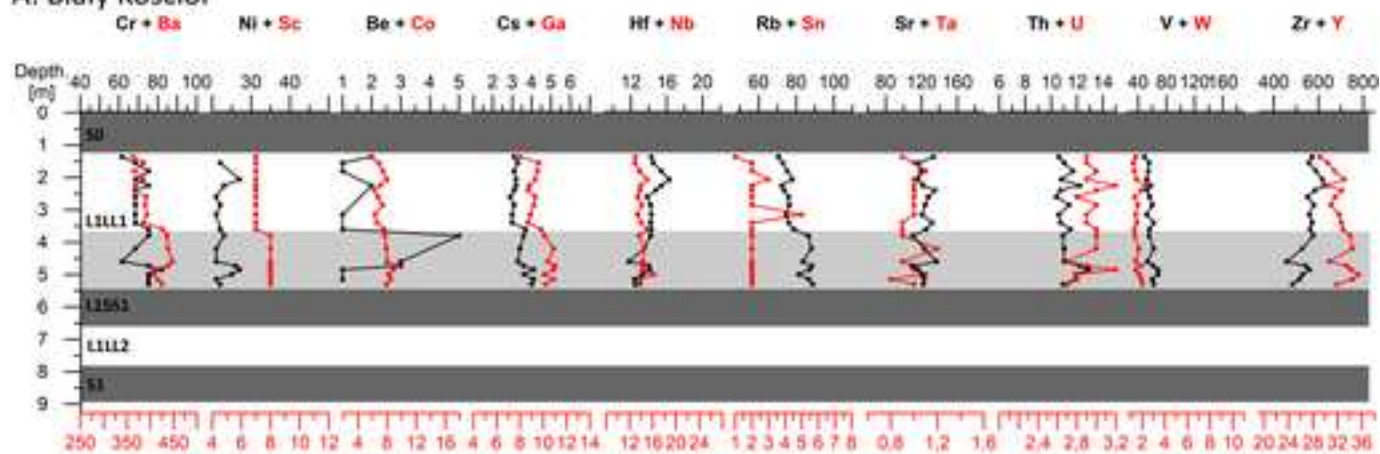
B. Złota



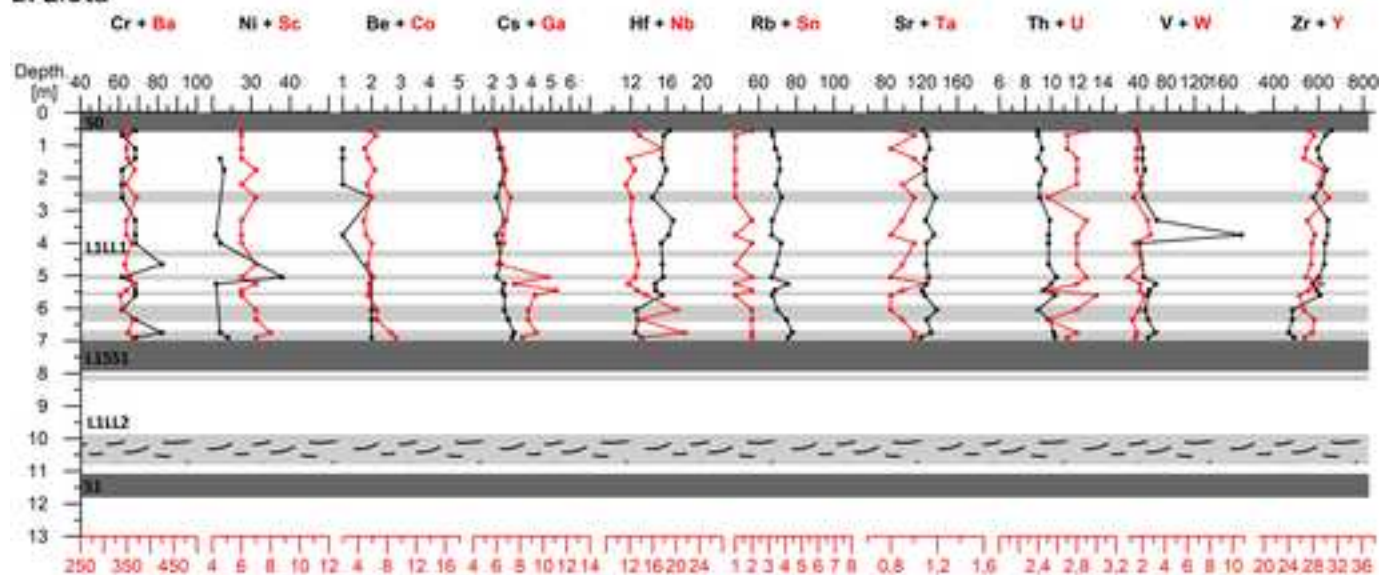
C. Tyszowce



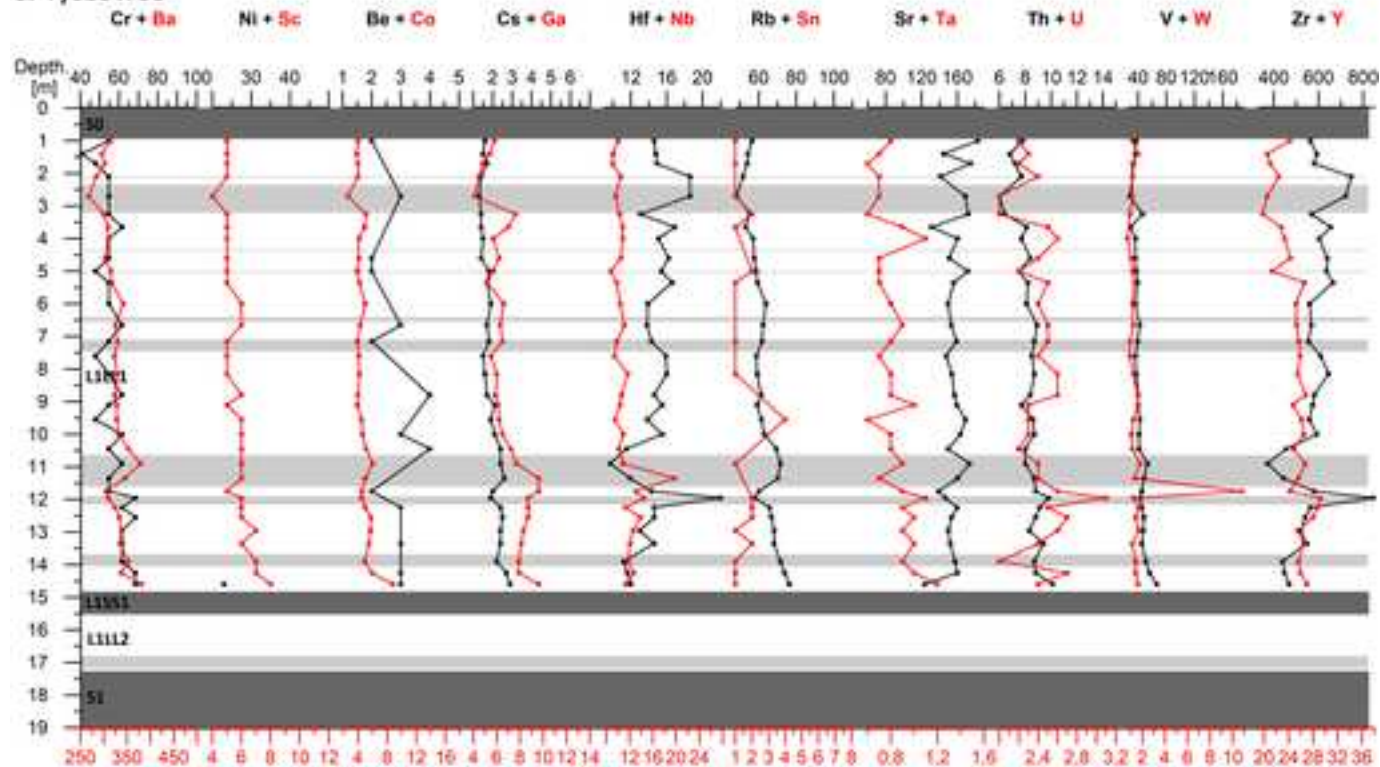
A. Biały Kościół



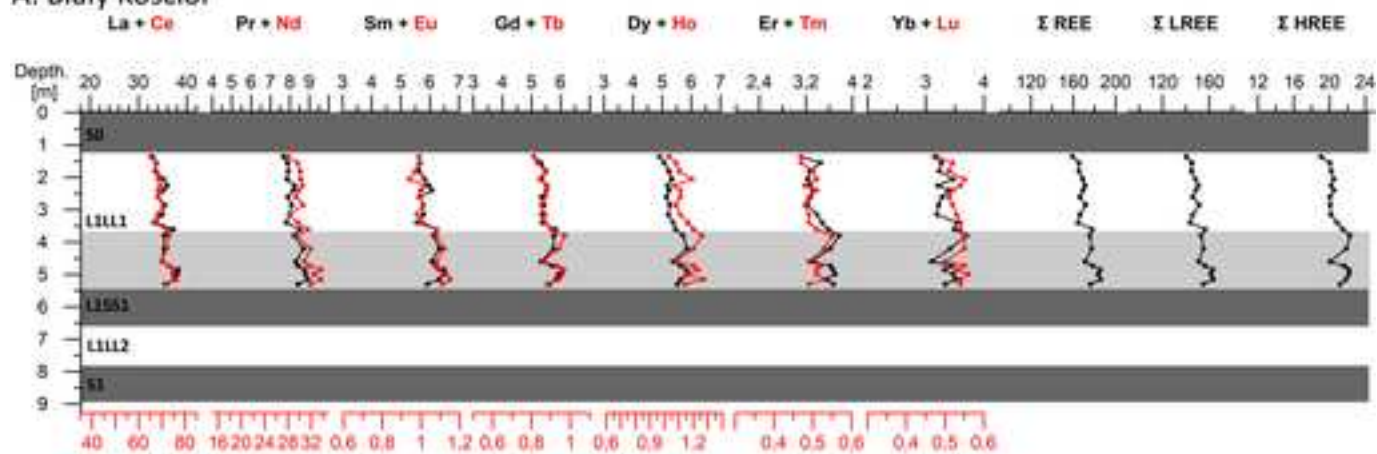
B. Złota



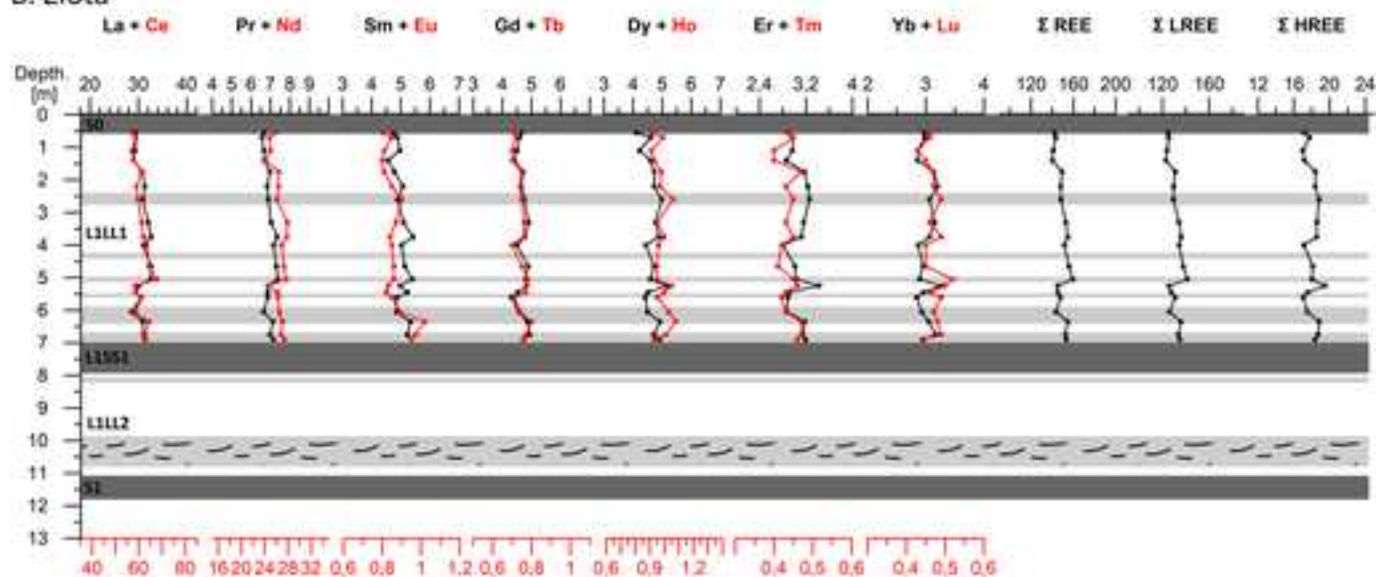
C. Tyszowce



A. Biały Kościół



B. Złota



C. Tyszowce

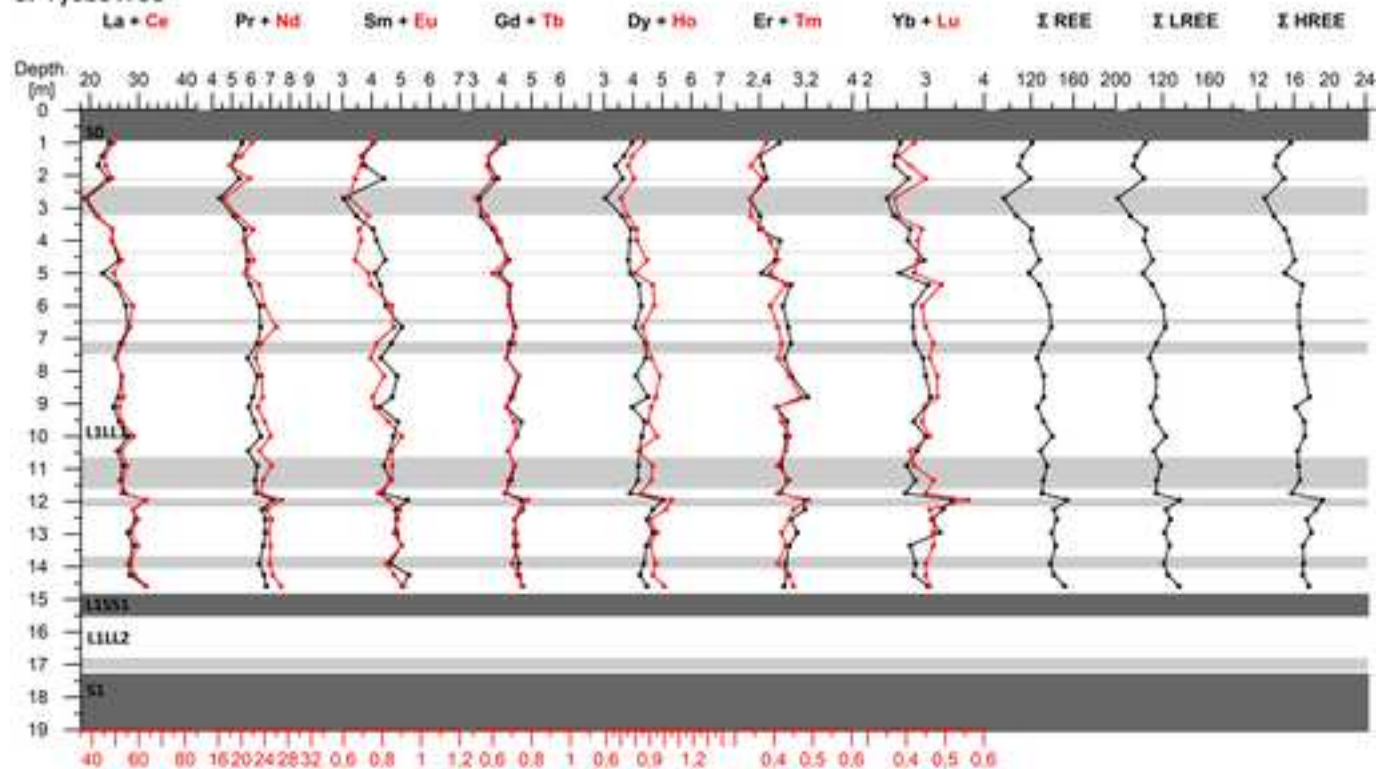
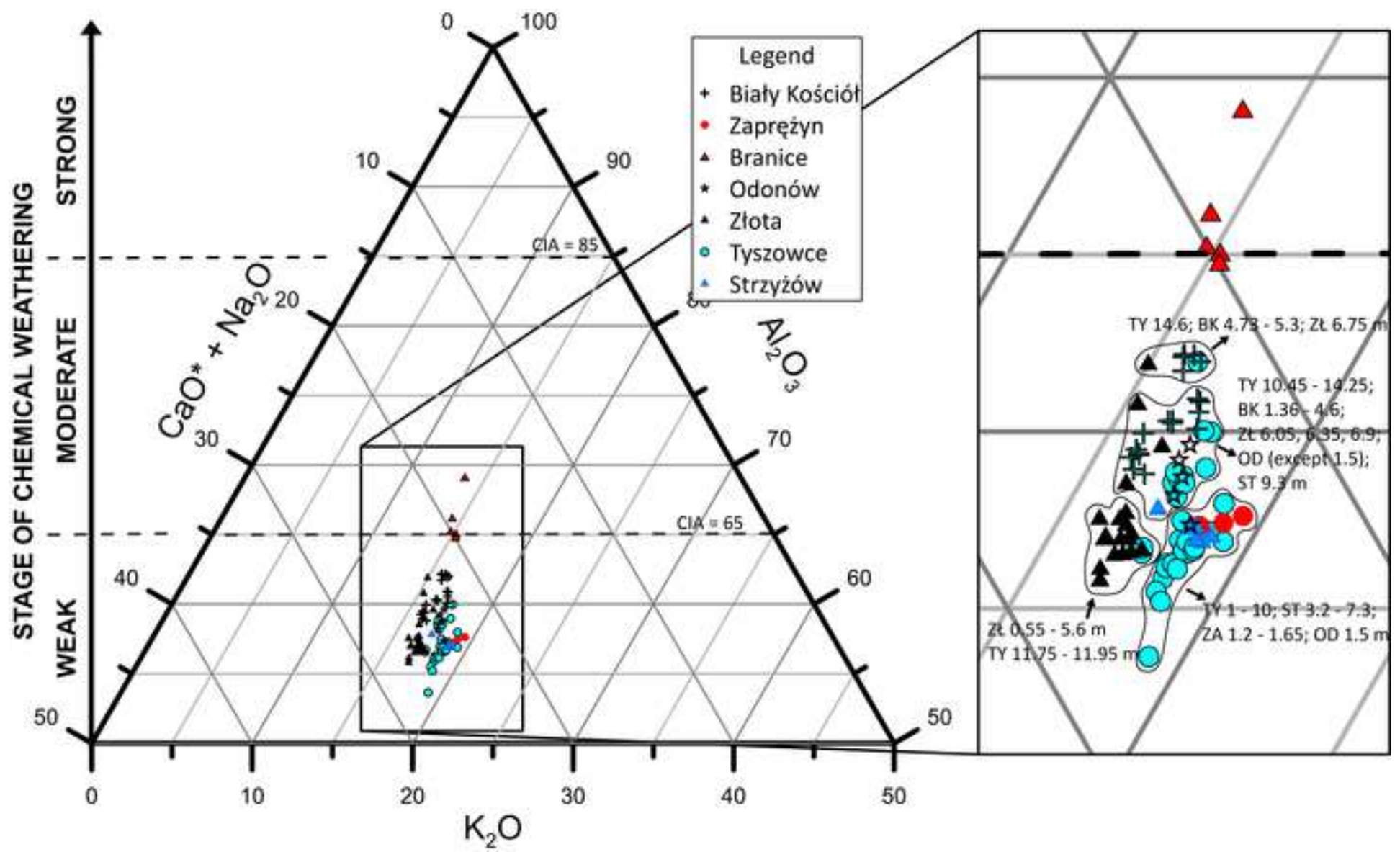
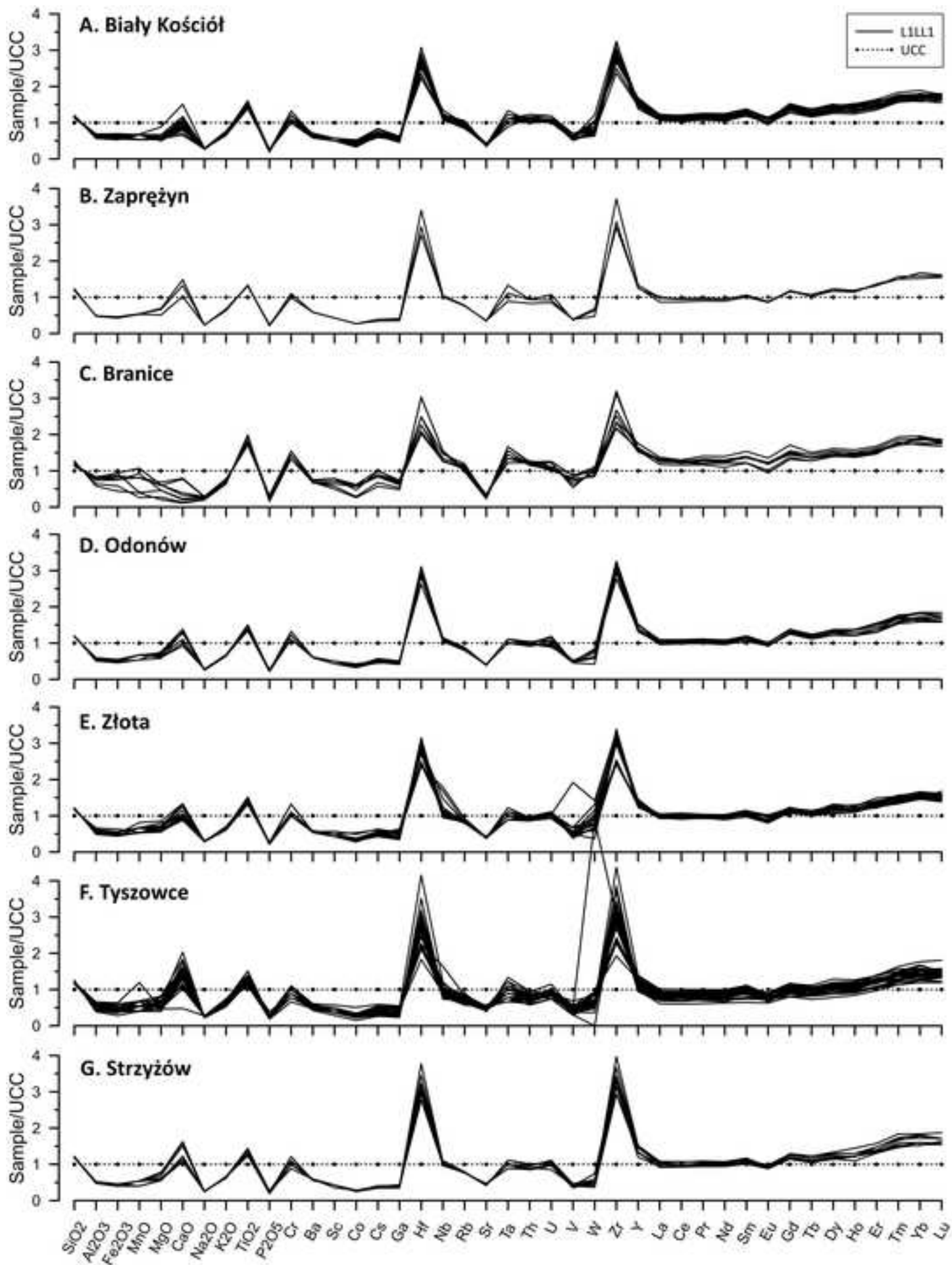


Figure 6





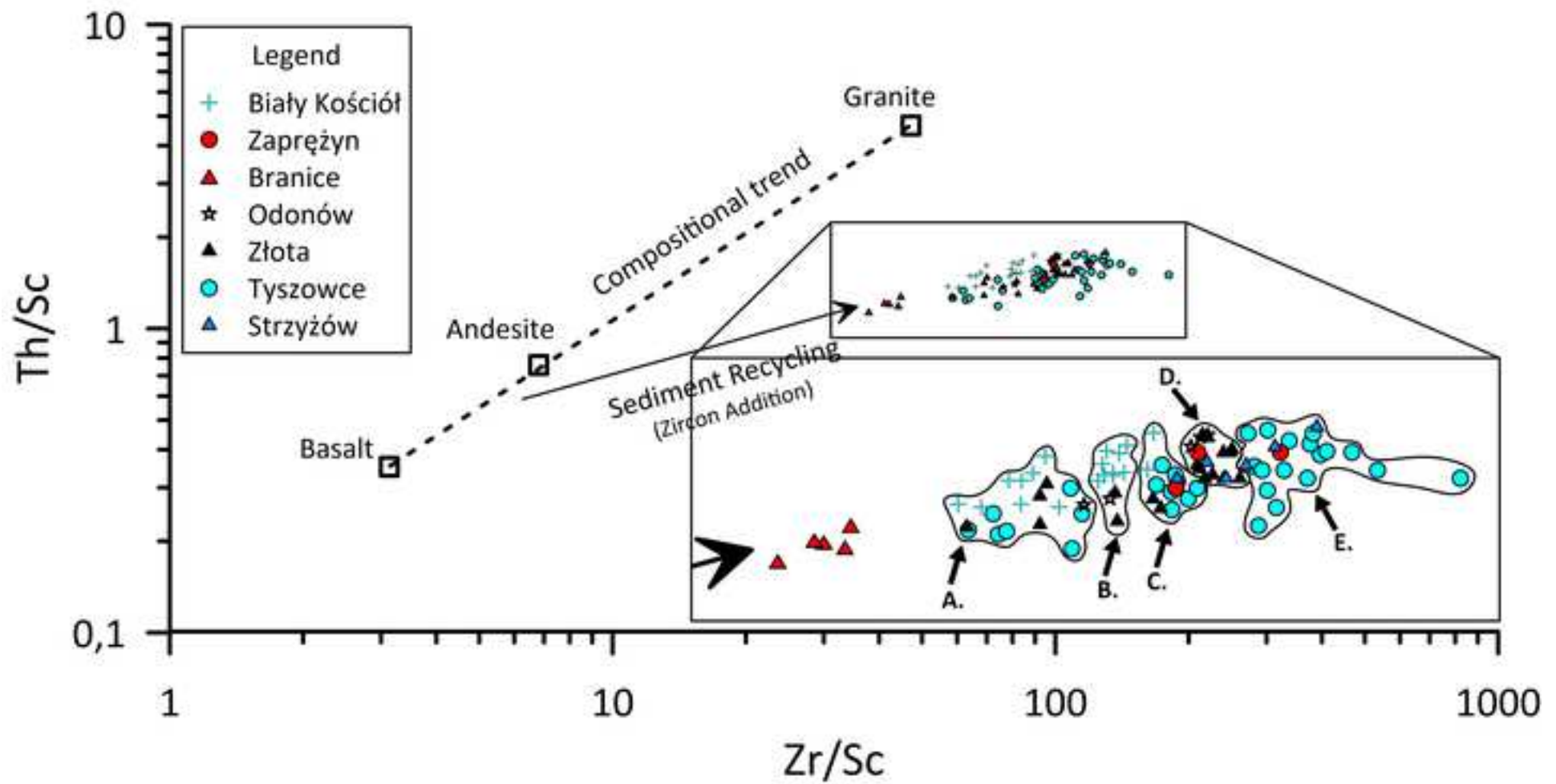
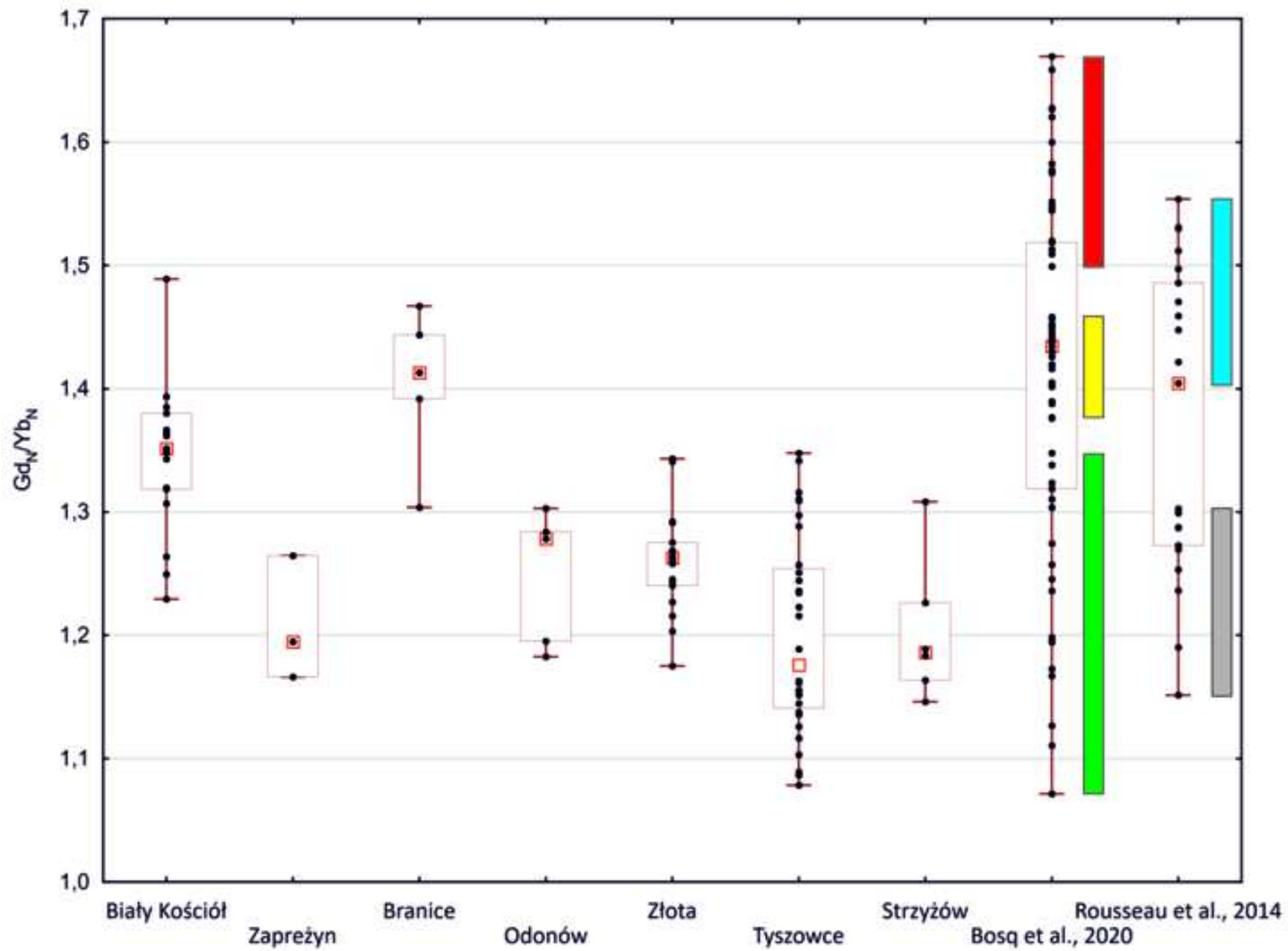
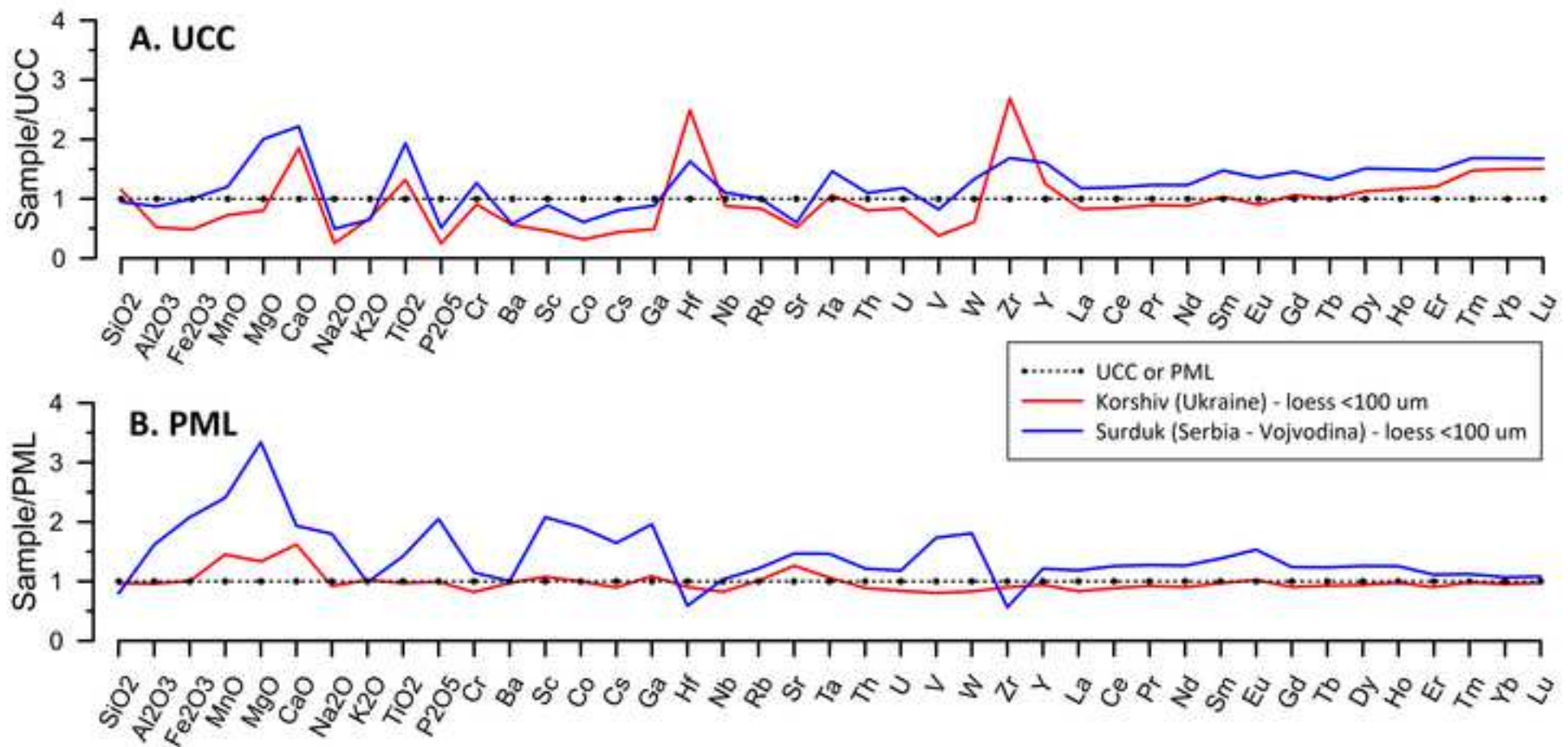


Figure 9





Implications of the geochemistry of L1LL1 (MIS2) loess in Poland for paleoenvironment and new normalizing values for loess-focused multi-elemental analyses

Supplementary figures

Fig. S1. The variability of granulometric composition (divided into individual fractions) at Biały Kościół (A), Złota (B) and Tyszowce (C). The main pedo- and lithostratigraphic units are shown. Legend of lithological markings consistent with Fig. 2.

Fig. S2. Shepard's (1954) triangular diagram, based on Wentworth's (1922) classification, for the supplementary research sites.

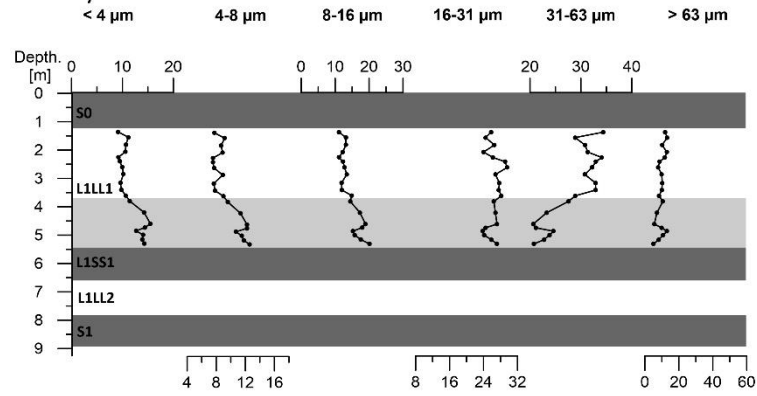
Fig. S3. A-CN-K ternary diagram (Nesbitt and Young, 1984) of the Złota loess-palaeosol samples (after Skurzyński et al., 2020, modified). CaO* (Ca in silicates) was calculated according to McLennan (1993). Dashed lines – CIA values of 65 and 85. Stratigraphical labelling system after Kukla and An (1989), modified by Marković et al. (2008, 2015). U.M.* means “underlying material”.

Fig. S4. A-CN-K ternary diagram (Nesbitt and Young, 1984) of the Biały Kościół samples. Only L1LL1 loess is shown. CaO* (Ca in silicates) was calculated according to McLennan (1993). Dashed lines – CIA values of 65 and 85. Stratigraphical labelling system after Kukla and An (1989), modified by Marković et al. (2008, 2015).

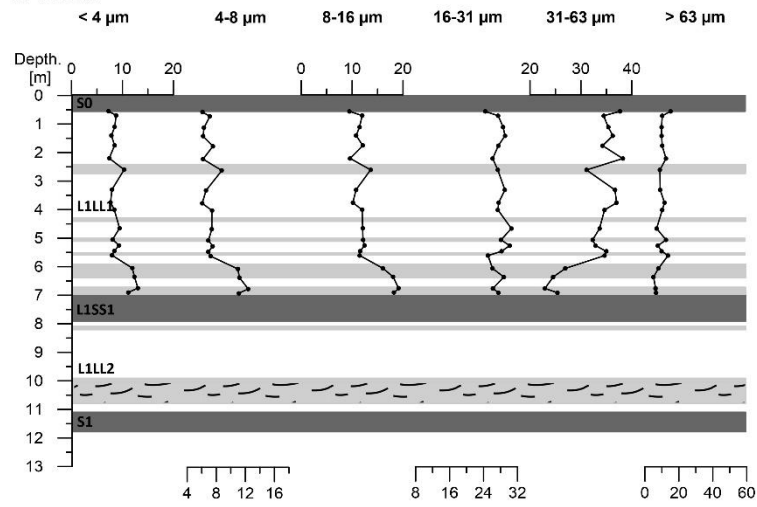
Fig. S5. A-CN-K ternary diagram (Nesbitt and Young, 1984) of the Tyszowce samples. Only L1LL1 loess is shown. CaO* (Ca in silicates) was calculated according to McLennan (1993). Dashed lines – CIA values of 65 and 85. Stratigraphical labelling system after Kukla and An (1989), modified by Marković et al. (2008, 2015).

Table S1. Method detection limits (MDL) and precision (RSD – relative standard deviation) for investigated elements and oxides. RSD was presented separately for each of the four independent measurement series, based on the analysis of the same standard STD SO-19 (Biały Kościół, i.e. BK - 6; Złota, i.e. ZŁ - 5; Tyszowce, i.e. TY - 10; Zaprężyn, Strzyżów, Odonów and Branice, i.e. Z+S+O+B - 3 markings). The RSD value should be understood as the percentage average deviation from the mean value (e.g. 60.40 ± 0.18 means that the standard deviation is $\pm 0.18\%$ of the mean value of 60.40%). The results are presented in the form obtained from an external laboratory, i.e. major elements and chromium are converted to oxides and expressed in wt%, trace elements and rare earth elements are presented in ppm.

A. Biały Kościół



B. Żłota



C. Tyszowce

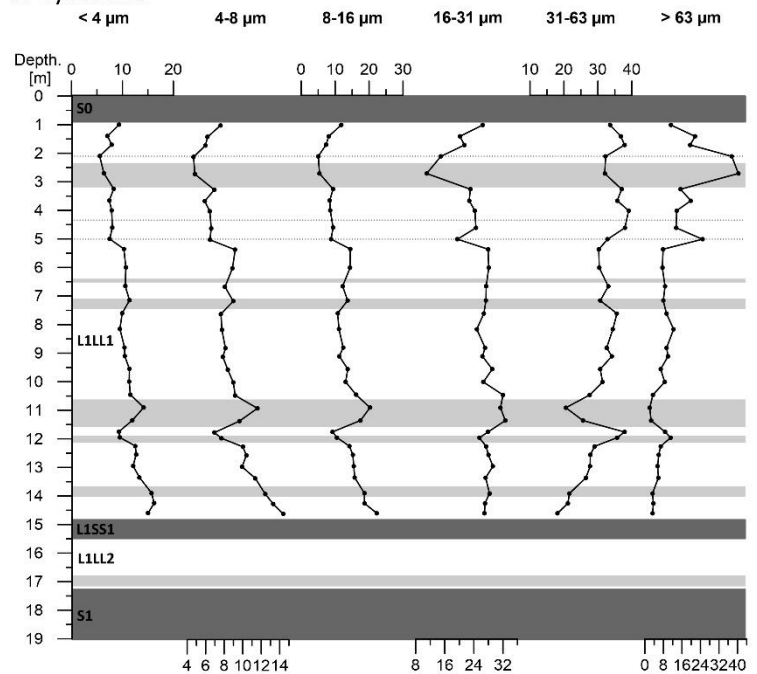


Fig. S1. The variability of granulometric composition (divided into individual fractions) at Biały Kościół (A), Żłota (B) and Tyszowce (C). The main pedo- and lithostratigraphic units are shown. Legend of lithological markings consistent with Fig. 2.

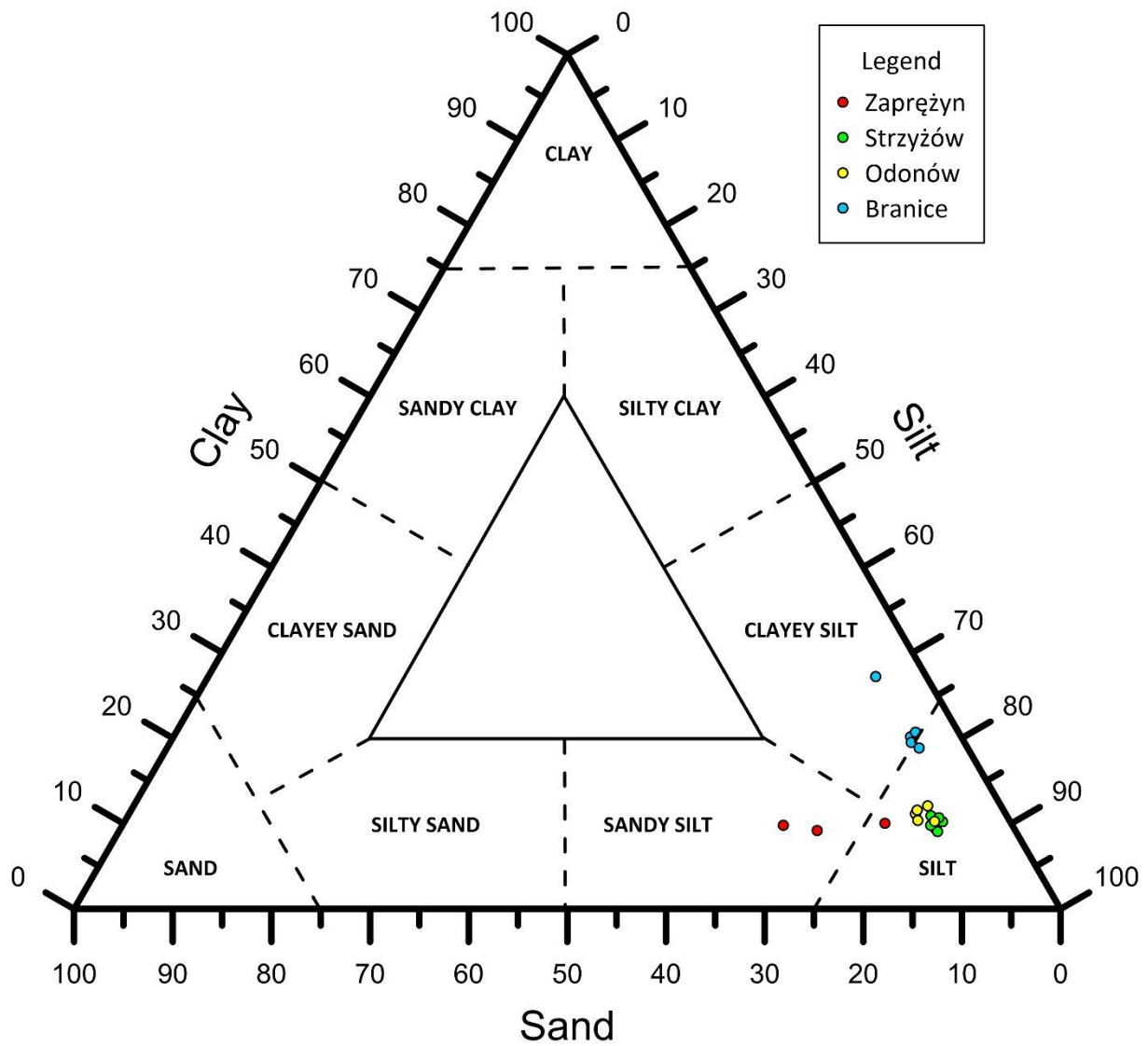


Fig. S2. Shepard's (1954) triangular diagram, based on Wentworth's (1922) classification, for the supplementary research sites.

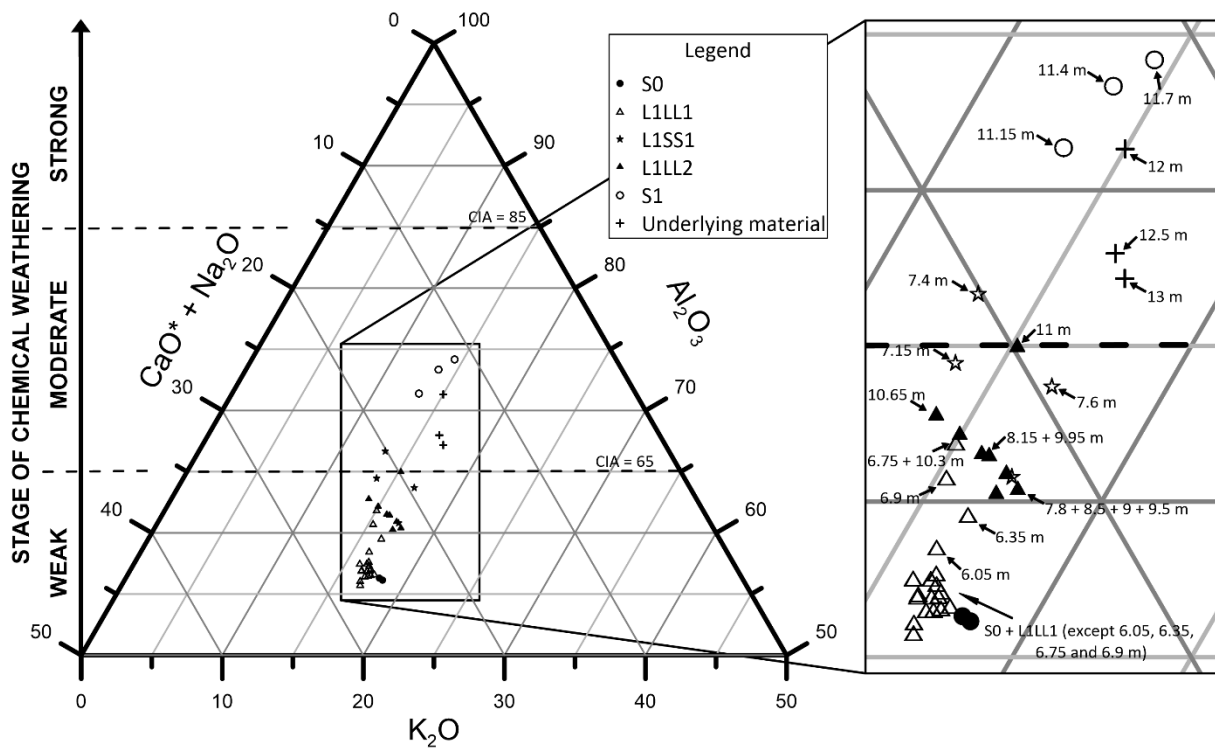


Fig. S3. A-CN-K ternary diagram (Nesbitt and Young, 1984) of the Złota loess-palaeosol samples (after Skurzyński et al., 2020, modified). CaO* (Ca in silicates) was calculated according to McLennan (1993). Dashed lines – CIA values of 65 and 85. Stratigraphical labelling system after Kukla and An (1989), modified by Marković et al. (2008, 2015). U.M.* means “underlying material”.

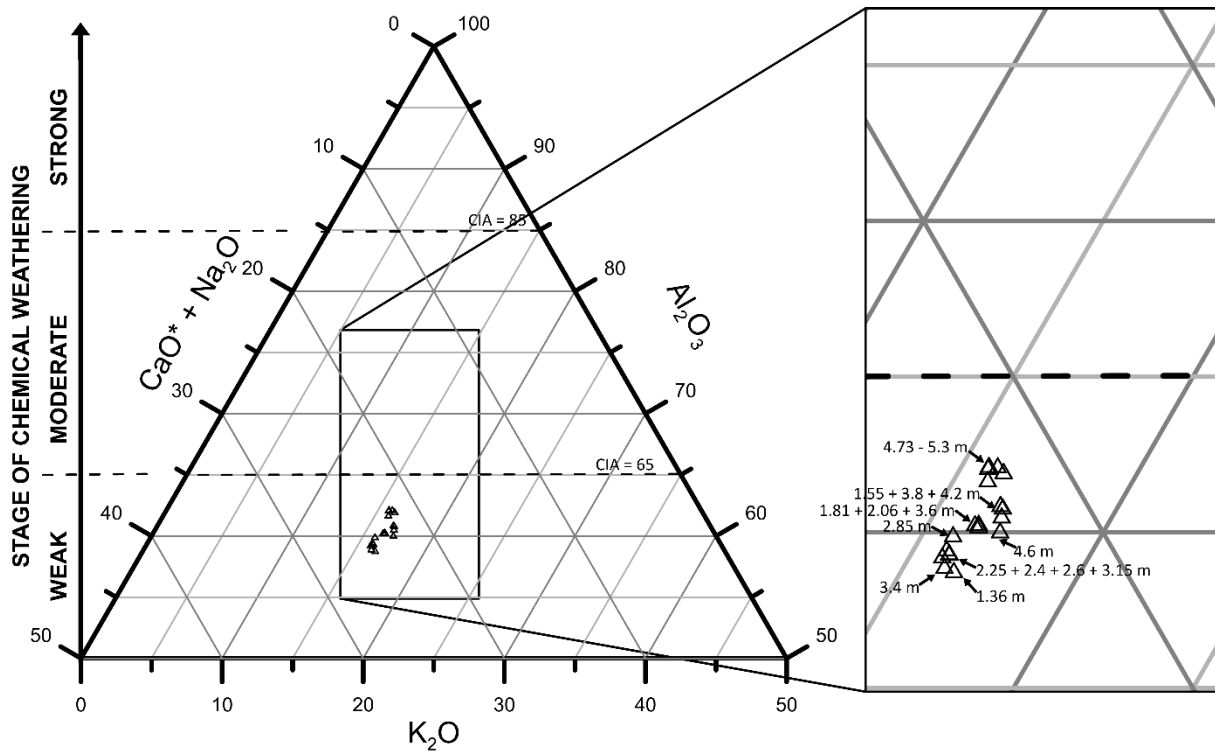


Fig. S4. A-CN-K ternary diagram (Nesbitt and Young, 1984) of the Biały Kościół samples. Only L1LL1 loess is shown. CaO* (Ca in silicates) was calculated according to McLennan (1993). Dashed lines – CIA values of 65 and 85. Stratigraphical labelling system after Kukla and An (1989), modified by Marković et al. (2008, 2015).

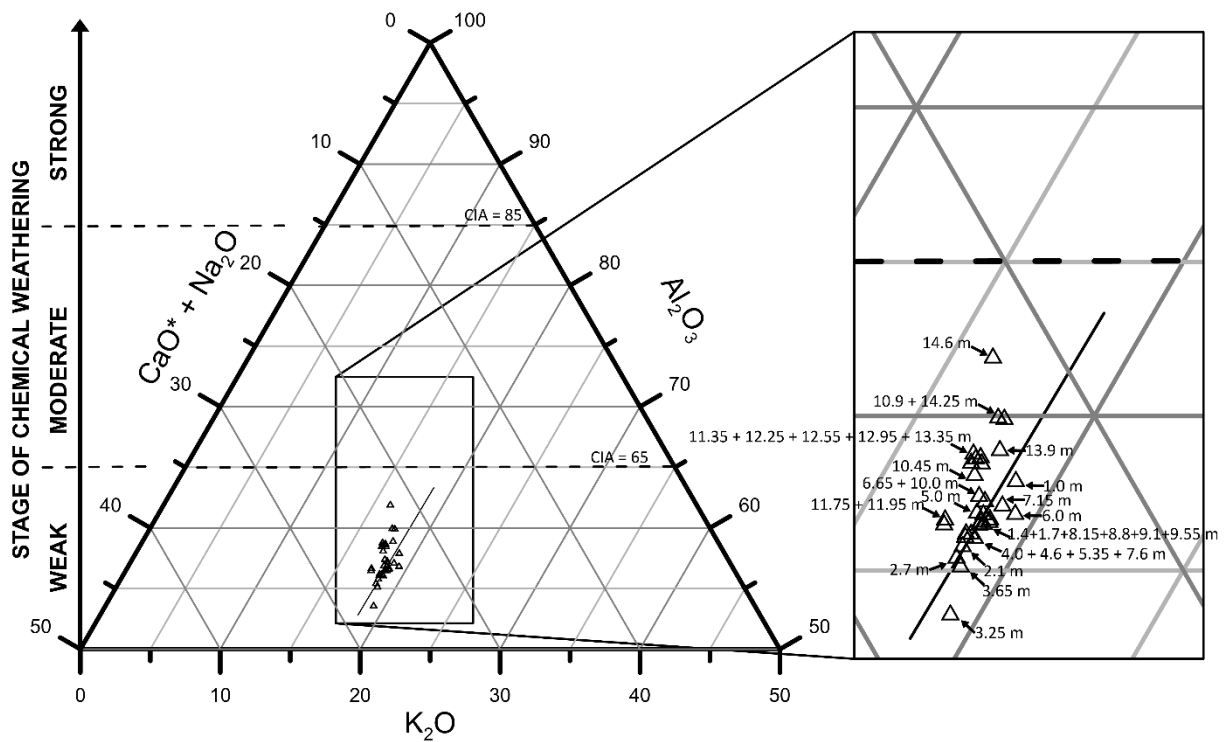


Fig. S5. A-CN-K ternary diagram (Nesbitt and Young, 1984) of the Tyszowce samples. Only L1LL1 loess is shown. CaO* (Ca in silicates) was calculated according to McLennan (1993). Dashed lines – CIA values of 65 and 85. Stratigraphical labelling system after Kukla and An (1989), modified by Marković et al. (2008, 2015).

Table S1. Method detection limits (MDL) and precision (RSD – relative standard deviation) for investigated elements and oxides. RSD was presented separately for each of the four independent measurement series, based on the analysis of the same standard STD SO-19 (Biały Kościół, i.e. BK - 6; Złota, i.e. Zł - 5; Tyszowce, i.e. TY - 10; Zapreżyn, Strzyżów, Odonów and Branice, i.e. Z+S+O+B - 3 markings). The RSD value should be understood as the percentage average deviation from the mean value (e.g. 60.40 ± 0.18 means that the standard deviation is ± 0.18% of the mean value of 60.40%). The results are presented in the form obtained from an external laboratory, i.e. major elements and chromium are converted to oxides and expressed in wt%, trace elements and rare earth elements are presented in ppm.

	AVERAGE VALUE ± RSD (%)							AVERAGE VALUE ± RSD (%)					
	MDL	STD SO-19	BK	ZŁ	TY	Z+S+O+B		MDL	STD SO-19	BK	ZŁ	TY	Z+S+O+B
SiO ₂ %	0,010	61,13	60,56 ± 0,12	60,30 ± 0,22	60,40 ± 0,18	60,31 ± 0,09	Sr	0,50	317,10	314,08 ± 3,29	316,46 ± 0,96	324,11 ± 1,29	315,27 ± 2,16
Al ₂ O ₃ %	0,010	13,95	13,91 ± 0,35	13,98 ± 0,57	14,00 ± 0,41	14,03 ± 0,06	Ta	0,10	4,90	4,42 ± 4,79	4,86 ± 3,59	4,73 ± 4,83	5,03 ± 1,87
Fe ₂ O ₃ %	0,040	7,47	7,45 ± 0,80	7,50 ± 0,82	7,45 ± 0,58	7,51 ± 0,70	Th	0,20	13,00	13,42 ± 2,84	13,28 ± 2,10	12,85 ± 3,60	13,97 ± 2,43
MnO %	0,010	0,13	0,13 ± 0,00	0,13 ± 0,00	0,13 ± 0,00	0,13 ± 0,00	U	0,10	19,40	19,53 ± 1,44	19,56 ± 2,18	20,11 ± 2,13	20,87 ± 2,16
MgO %	0,010	2,88	2,93 ± 1,31	2,92 ± 0,59	2,91 ± 1,04	2,92 ± 0,28	V	8,00	165,00	165,17 ± 1,90	170,40 ± 2,31	167,70 ± 3,04	169,67 ± 2,00
CaO %	0,010	6,00	5,97 ± 0,72	5,97 ± 0,84	5,92 ± 0,82	5,95 ± 0,00	W	0,50	9,80	9,93 ± 5,92	10,54 ± 9,40	9,66 ± 5,88	9,77 ± 3,38
Na ₂ O %	0,010	4,11	4,01 ± 1,50	4,07 ± 1,29	4,09 ± 1,56	4,04 ± 0,84	Zr	0,10	112,00	112,53 ± 2,59	109,34 ± 1,31	109,44 ± 1,71	113,47 ± 2,73
K ₂ O %	0,010	1,29	1,26 ± 3,21	1,32 ± 1,14	1,31 ± 0,77	1,30 ± 0,73	Y	0,10	35,50	36,32 ± 3,81	35,00 ± 2,04	35,38 ± 2,04	37,13 ± 3,30
TiO ₂ %	0,010	0,69	0,70 ± 0,00	0,70 ± 0,70	0,70 ± 0,64	0,70 ± 0,00	La	0,10	71,30	71,35 ± 1,78	72,42 ± 2,31	71,53 ± 1,94	74,43 ± 2,91
P ₂ O ₅ %	0,010	0,32	0,32 ± 3,32	0,32 ± 3,70	0,33 ± 2,06	0,32 ± 1,46	Ce	0,10	161,00	157,52 ± 1,01	158,66 ± 1,34	159,78 ± 1,37	166,43 ± 3,10
Cr ₂ O ₃ %	0,002	0,50	0,49 ± 0,43	0,50 ± 1,21	0,50 ± 0,87	0,51 ± 0,16	Pr	0,02	19,40	19,40 ± 2,28	19,06 ± 1,44	18,99 ± 1,52	20,34 ± 2,40
Ba	1,000	486,00	470,83 ± 1,53	460,80 ± 1,40	458,30 ± 2,13	471,67 ± 1,39	Nd	0,30	75,70	74,40 ± 2,67	74,30 ± 1,15	74,33 ± 2,91	78,67 ± 2,73
Ni	20,000	470,00	471,50 ± 1,56	475,00 ± 1,58	462,60 ± 1,32	482,33 ± 0,54	Sm	0,05	13,70	13,12 ± 2,78	12,89 ± 1,71	12,95 ± 1,50	13,44 ± 2,80
Sc	1,000	27,00	26,33 ± 1,79	26,80 ± 3,66	26,50 ± 2,53	27,00 ± 0,00	Eu	0,02	3,81	3,64 ± 2,56	3,58 ± 2,86	3,61 ± 2,18	3,82 ± 2,14
Be	1,000	20,00	13,50 ± 34,41	19,80 ± 26,80	17,80 ± 16,27	19,67 ± 4,79	Gd	0,05	10,53	10,60 ± 1,56	10,13 ± 1,39	10,19 ± 1,70	10,81 ± 1,70
Co	0,200	24,00	23,85 ± 4,59	23,70 ± 2,96	23,56 ± 2,71	23,97 ± 2,75	Tb	0,01	1,41	1,39 ± 1,55	1,34 ± 1,60	1,34 ± 1,79	1,43 ± 2,82
Cs	0,100	4,50	4,45 ± 4,81	4,32 ± 8,33	4,14 ± 7,88	4,60 ± 3,07	Dy	0,05	7,50	7,40 ± 1,82	7,26 ± 2,09	7,17 ± 2,26	7,53 ± 1,79
Ga	0,500	17,50	16,48 ± 6,23	15,80 ± 3,90	16,47 ± 6,29	15,93 ± 1,48	Ho	0,02	1,39	1,36 ± 2,61	1,34 ± 1,11	1,33 ± 2,69	1,41 ± 2,98
Hf	0,100	3,10	3,12 ± 6,79	3,08 ± 2,43	3,05 ± 5,34	3,23 ± 3,86	Er	0,03	3,78	3,88 ± 2,28	3,75 ± 3,51	3,77 ± 3,45	4,04 ± 1,34
Nb	0,100	68,50	70,87 ± 2,39	68,24 ± 1,67	68,66 ± 1,58	71,83 ± 1,93	Tm	0,01	0,55	0,52 ± 3,29	0,51 ± 3,61	0,52 ± 3,26	0,56 ± 2,92
Rb	0,100	19,50	19,35 ± 3,10	20,20 ± 4,78	19,67 ± 2,35	20,00 ± 2,55	Yb	0,05	3,55	3,38 ± 4,56	3,36 ± 3,06	3,36 ± 3,91	3,55 ± 2,13
Sn	1,000	19,00	17,83 ± 3,85	17,80 ± 2,25	17,80 ± 4,90	19,33 ± 2,44	Lu	0,01	0,53	0,51 ± 3,84	0,50 ± 4,56	0,50 ± 3,27	0,55 ± 2,57

Table S2. Geochemical composition of the Polish loess. Major elements (wt%) are recalculated on a volatile-free basis.

Research Site	Depth (m b.g.l)	LOI	OXIDES OF MAJOR ELEMENTS							
			SiO ₂	Al ₂ O ₃	Fe ₂ O ₃	MgO	CaO	Na ₂ O	K ₂ O	TiO ₂
BIAŁY KOŚCIÓŁ	1.36	6.20	78.81	8.60	2.65	1.10	4.68	1.10	2.22	0.69
	1.55	6.30	78.11	9.19	3.01	1.21	4.26	1.03	2.34	0.72
	1.81	5.60	78.56	9.31	2.98	1.21	3.61	1.09	2.34	0.75
	2.06	5.30	79.26	9.16	2.78	1.10	3.42	1.08	2.31	0.75
	2.25	5.70	78.77	9.11	2.77	1.18	3.85	1.15	2.27	0.76
	2.40	6.40	78.10	8.91	2.77	1.34	4.65	1.14	2.21	0.75
	2.60	5.80	78.48	9.23	2.79	1.26	3.92	1.16	2.28	0.75
	2.85	5.60	78.75	9.26	2.89	1.22	3.59	1.14	2.26	0.75
	3.15	5.60	79.17	9.03	2.75	1.19	3.60	1.14	2.25	0.73
	3.40	6.00	78.43	9.03	2.76	1.28	4.17	1.16	2.28	0.74
	3.60	6.10	78.01	9.58	2.96	1.31	3.72	1.13	2.39	0.76
	3.80	5.20	79.02	9.66	2.95	1.24	2.76	1.08	2.44	0.73
	4.20	7.00	75.99	9.90	3.15	1.47	4.93	1.12	2.55	0.74
	4.60	8.50	73.97	9.95	3.12	1.94	6.35	1.15	2.62	0.74
	4.73	6.10	77.29	10.49	3.27	1.36	2.99	1.12	2.54	0.79
	4.85	6.40	76.68	10.32	3.48	1.34	3.67	1.10	2.45	0.80
	4.99	6.90	76.25	10.27	3.35	1.33	4.36	1.11	2.40	0.79
5.15	6.40	76.77	10.47	3.36	1.35	3.53	1.14	2.45	0.77	
5.30	6.00	76.87	10.46	3.46	1.29	3.34	1.15	2.50	0.79	
ZAPRĘŻYN	1.20	7.30	78.51	7.42	2.30	1.52	6.24	0.90	2.31	0.66
	1.50	6.70	79.35	7.42	2.21	1.46	5.57	0.92	2.28	0.66
	1.65	5.50	81.36	7.21	2.14	1.12	4.29	0.92	2.15	0.67
BRANICE	1.26	7.10	74.71	11.92	4.12	1.31	3.24	1.10	2.57	0.87
	1.54	7.50	74.37	12.18	3.79	1.51	3.34	1.14	2.65	0.87
	1.75	6.50	75.42	12.61	4.27	1.33	1.64	1.12	2.53	0.91
	1.96	6.30	75.36	12.41	4.70	1.34	1.35	1.16	2.59	0.89
	2.38	6.50	76.50	12.65	4.61	1.01	0.85	0.98	2.32	0.96
ODONÓW	0.90	7.00	78.59	8.19	2.47	1.27	5.51	0.97	2.18	0.70
	1.50	7.10	78.51	7.69	2.28	1.67	5.80	0.99	2.26	0.67
	1.80	6.80	78.29	8.30	2.45	1.52	5.41	1.01	2.21	0.68
	2.50	7.40	77.53	8.41	2.52	1.56	5.80	1.04	2.31	0.68
	3.30	6.90	77.99	8.38	2.43	1.60	5.35	1.07	2.32	0.70
ZŁOTA	0.55	5.50	80.99	7.40	2.20	1.22	4.22	1.10	2.07	0.66
	0.70	5.60	80.52	7.70	2.23	1.21	4.29	1.08	2.17	0.66
	1.10	6.60	78.50	7.88	2.30	1.60	5.56	1.09	2.24	0.67
	1.40	5.60	80.03	7.85	2.27	1.31	4.42	1.12	2.19	0.68
	1.75	5.40	80.21	7.92	2.39	1.28	4.08	1.10	2.18	0.68
	2.20	5.60	80.26	7.72	2.32	1.31	4.32	1.14	2.12	0.66
	2.60	6.60	78.66	8.09	2.33	1.48	5.28	1.12	2.22	0.67
	3.30	5.70	80.04	7.96	2.44	1.26	4.20	1.12	2.17	0.69
	3.75	6.10	79.36	7.90	2.27	1.46	4.85	1.13	2.18	0.70
	4.00	5.80	80.28	7.98	2.29	1.33	4.03	1.10	2.15	0.69
	4.65	5.60	80.19	7.99	2.41	1.31	3.98	1.14	2.12	0.71
	5.05	5.40	80.17	8.22	2.46	1.24	3.74	1.17	2.18	0.70
	5.25	5.50	79.71	8.57	2.26	1.34	3.81	1.18	2.27	0.71
	5.45	5.20	80.40	8.26	2.27	1.28	3.67	1.12	2.19	0.68
	5.60	5.40	80.25	8.25	2.29	1.31	3.81	1.15	2.12	0.69
	6.05	7.40	76.55	9.05	2.56	1.88	5.61	1.19	2.31	0.69
	6.35	6.90	77.37	9.35	2.74	1.77	4.37	1.14	2.39	0.71
6.75	7.50	76.56	10.02	3.18	1.53	4.43	1.14	2.24	0.76	
6.90	6.90	78.23	9.44	2.82	1.44	3.87	1.13	2.20	0.73	
	1.00	8.80	76.86	7.22	2.10	1.41	8.54	0.88	2.17	0.64
	1.40	5.90	82.19	6.59	1.78	0.96	4.92	0.88	1.99	0.57
	1.70	7.70	79.26	6.68	1.84	1.23	7.35	0.89	2.03	0.59
	2.10	5.80	81.94	6.37	1.74	1.02	5.34	0.89	1.93	0.63
	2.70	6.30	82.65	5.90	1.41	0.87	5.83	0.84	1.81	0.59
	3.25	7.10	80.19	6.65	1.78	1.19	6.30	1.02	2.19	0.55
	3.65	6.60	80.95	6.71	1.86	1.32	5.35	0.97	2.09	0.61
	4.00	6.40	80.54	6.93	1.84	1.16	5.76	0.95	2.08	0.62
	4.60	6.30	80.62	6.96	1.93	1.18	5.48	0.96	2.10	0.64
	5.00	6.50	80.66	6.95	1.91	1.07	5.71	0.92	2.06	0.60
	5.35	6.60	80.15	7.13	2.02	1.23	5.56	0.98	2.16	0.65
	6.00	7.70	77.56	7.61	2.20	1.77	6.73	0.97	2.39	0.64
	6.65	6.80	79.36	7.56	2.17	1.32	5.62	0.98	2.22	0.66

TYSZOWCE	7.15	7.90	77.78	7.51	2.15	1.71	6.81	0.96	2.29	0.65
	7.60	7.10	79.23	7.09	1.97	1.50	6.30	0.97	2.17	0.64
	8.15	7.10	79.18	7.20	2.05	1.40	6.26	0.96	2.17	0.66
	8.80	7.20	78.66	7.53	2.16	1.48	6.13	0.99	2.26	0.65
	9.10	7.30	78.64	7.37	2.10	1.45	6.45	0.97	2.25	0.64
	9.55	8.40	76.37	7.65	2.30	1.81	7.70	1.01	2.33	0.67
	10.00	7.40	78.07	7.77	2.28	1.35	6.46	1.01	2.25	0.66
	10.45	6.40	78.73	8.52	2.49	1.34	4.68	1.08	2.38	0.65
	10.90	8.30	75.62	9.09	2.73	1.51	6.74	1.04	2.45	0.66
	11.35	7.40	77.49	8.60	2.52	1.41	5.77	1.06	2.36	0.66
	11.75	5.60	81.29	7.39	2.07	1.04	4.31	1.03	2.11	0.64
	11.95	6.10	80.93	7.18	2.10	1.12	4.73	0.99	2.04	0.76
	12.25	7.60	78.01	8.12	2.43	1.24	6.15	1.02	2.21	0.68
	12.55	6.90	78.38	8.41	2.42	1.24	5.37	1.04	2.29	0.70
	12.95	6.40	78.60	8.74	2.49	1.28	4.62	1.08	2.36	0.70
	13.35	6.40	78.90	8.46	2.51	1.32	4.59	1.05	2.35	0.69
	13.90	8.20	75.75	9.05	2.77	1.76	6.22	1.08	2.53	0.67
14.25	8.00	75.93	9.29	3.02	1.55	5.81	1.07	2.47	0.70	
14.60	5.60	79.37	10.00	3.16	1.03	2.01	1.07	2.41	0.75	
STRZYŻÓW	3.20	6.10	80.68	7.39	2.01	1.22	4.81	0.95	2.20	0.64
	3.80	7.60	78.36	7.27	2.07	1.66	6.73	0.94	2.22	0.62
	4.40	7.40	79.03	7.22	1.98	1.53	6.35	0.94	2.19	0.63
	5.00	7.90	77.96	7.40	2.13	1.70	6.84	0.95	2.27	0.62
	7.30	7.90	77.83	7.55	2.15	1.72	6.72	0.98	2.23	0.67
	9.30	6.70	79.78	7.63	2.27	1.26	5.16	1.00	2.11	0.70

*Implications of the geochemistry of L1LL1 (MIS2) loess in Poland for paleoenvironment and new normalizing values for loess-focused multi-element. The color scale was developed using the Conditional Formatting function of MS Excel - the red-yellow-green color scale indicates the position of a

Table S3. Basic statistics of geochemical composition of the Polish loess. Major elements (wt%) are recalculated or

Basic Statistic	Research Site	LOI	OXIDES OF MAJOR ELEMENTS							
			SiO ₂	Al ₂ O ₃	Fe ₂ O ₃	MgO	CaO	Na ₂ O	K ₂ O	TiO ₂
MEDIAN	Biały Kościół	6.10	78.11	9.31	2.96	1.28	3.72	1.13	2.34	0.75
	Złota	5.60	80.04	7.99	2.32	1.31	4.22	1.13	2.18	0.69
	Tyszowce	7.00	79.04	7.45	2.13	1.32	5.79	0.99	2.22	0.65
	Zaprężyń	6.70	79.35	7.42	2.21	1.46	5.57	0.92	2.28	0.66
	Branice	6.50	75.36	12.41	4.27	1.33	1.64	1.12	2.57	0.89
	Odonów	7.00	78.29	8.30	2.45	1.56	5.51	1.01	2.26	0.68
	Strzyżów	7.50	78.69	7.39	2.10	1.59	6.54	0.95	2.21	0.63
AVERAGE	Biały Kościół	6.16	77.75	9.58	3.01	1.30	3.97	1.12	2.37	0.75
	Złota	6.02	79.38	8.29	2.42	1.40	4.34	1.13	2.20	0.69
	Tyszowce	6.99	79.06	7.63	2.20	1.32	5.80	0.99	2.21	0.65
	Zaprężyń	6.50	79.74	7.35	2.22	1.37	5.37	0.91	2.25	0.66
	Branice	6.78	75.27	12.35	4.30	1.30	2.08	1.10	2.53	0.90
	Odonów	7.04	78.18	8.19	2.43	1.52	5.57	1.02	2.26	0.69
	Strzyżów	7.27	78.94	7.41	2.10	1.51	6.10	0.96	2.20	0.65
MINIMUM	Biały Kościół	5.20	73.97	8.60	2.65	1.10	2.76	1.03	2.21	0.69
	Złota	5.20	76.55	7.40	2.20	1.21	3.67	1.08	2.07	0.66
	Tyszowce	5.60	75.62	5.90	1.41	0.87	2.01	0.84	1.81	0.55
	Zaprężyń	5.50	78.51	7.21	2.14	1.12	4.29	0.90	2.15	0.66
	Branice	6.30	74.37	11.92	3.79	1.01	0.85	0.98	2.32	0.87
	Odonów	6.80	77.53	7.69	2.28	1.27	5.35	0.97	2.18	0.67
	Strzyżów	6.10	77.83	7.22	1.98	1.22	4.81	0.94	2.11	0.62
MAXIMUM	Biały Kościół	8.50	79.26	10.49	3.48	1.94	6.35	1.16	2.62	0.80
	Złota	7.50	80.99	10.02	3.18	1.88	5.61	1.19	2.39	0.76
	Tyszowce	8.80	82.65	10.00	3.16	1.81	8.54	1.08	2.53	0.76
	Zaprężyń	7.30	81.36	7.42	2.30	1.52	6.24	0.92	2.31	0.67
	Branice	7.50	76.50	12.65	4.70	1.51	3.34	1.16	2.65	0.96
	Odonów	7.40	78.59	8.41	2.52	1.67	5.80	1.07	2.32	0.70
	Strzyżów	7.90	80.68	7.63	2.27	1.72	6.84	1.00	2.27	0.70
STANDARD DEV.	Biały Kościół	0.72	1.33	0.59	0.26	0.17	0.79	0.03	0.12	0.03
	Złota	0.71	1.31	0.67	0.24	0.18	0.57	0.03	0.07	0.03
	Tyszowce	0.84	1.83	0.94	0.38	0.23	1.14	0.06	0.16	0.04
	Zaprężyń	0.75	1.19	0.10	0.07	0.18	0.81	0.01	0.07	0.01
	Branice	0.45	0.73	0.27	0.33	0.16	1.02	0.06	0.12	0.04
	Odonów	0.21	0.39	0.26	0.08	0.14	0.19	0.03	0.06	0.01
	Strzyżów	0.66	1.02	0.14	0.10	0.20	0.81	0.02	0.05	0.03
MEDIAN	POLAND (n=89**)	6.50	78.64	8.19	2.41	1.32	4.81	1.07	2.25	0.68
AVERAGE		6.60	78.60	8.46	2.54	1.36	4.88	1.05	2.27	0.70
MINIMUM		5.20	73.97	5.90	1.41	0.87	0.85	0.84	1.81	0.55
MAXIMUM		8.80	82.65	12.65	4.70	1.94	8.54	1.19	2.65	0.96
STANDARD DEV.		0.86	1.78	1.41	0.61	0.21	1.38	0.09	0.15	0.07

*Implications of the geochemistry of L1LL1 (MIS2) loess in Poland for paleoenvironment and new normalizing values for loess-focused multi-element

**The number of samples for Ni and W is lower (n = 33 and 88, respectively).

The color scale was developed using the Conditional Formatting function of MS Excel - the red-yellow-green color scale indicates the position of a

Table S4. P-values of Shapiro-Wilk and Kruskal-Wallis tests for Polish loess.

Test	Research Site	LOI	OXIDES OF MAJOR ELEMENTS (P-values)							
			SiO ₂	Al ₂ O ₃	Fe ₂ O ₃	MgO	CaO	Na ₂ O	K ₂ O	TiO ₂
SHAPIRO-WILK*	Biały Kościół (n=19)	0.0086	0.01944	0.07583	0.07556	0.00015	0.04779	0.08360	0.31756	0.85000
	Złota (n=19***)	0.0042	0.00317	0.00635	0.00032	0.00340	0.01091	0.66501	0.26247	0.20185
	Tyszowce (n=32***)	0.5611	0.74385	0.23784	0.34668	0.58346	0.07445	0.17621	0.98553	0.27104
KRUSKAL-WALLIS**	Main Sites****		0.00480	0.00000	0.00000	0.25320	0.00000	0.00000	0.00010	0.00000

*P-values above 0.05 (marked in black) mean that the given variable has a distribution close to normal in a given main research site.

**P-values below 0.05 (marked in red) mean that at least one main research site differs significantly from the others in terms of the median of th

***Except the Ni (n = 15 in Biały Kościół, n = 8 in Złota, and n=1 in Tyszowce), and W (n=31 in Tyszowce).

****Main Sites i.e. Biały Kościół, Złota and Tyszowce. In the remaining research sites, the number of samples was less than the minimum require

given value in the entire range of values in a given column, separately for each statistical indicator (red = high values, green = low values).

		TRACE ELEMENTS (P-values)											
P ₂ O ₅	MnO	Cr	Ba	Ni	Sc	Co	Cs	Ga	Hf	Nb	Rb	Sr	Ta
0.01258	0.00002	0.01060	0.13428	0.00379	0.00001	0.95570	0.04058	0.41560	0.40916	0.25792	0.03959	0.68093	0.02275
0.00935	0.00007	0.00012	0.61260	0.00008	0.00008	0.00145	0.10613	0.01536	0.01197	0.00018	0.04109	0.14643	0.02189
0.00002	0.00000	0.00682	0.59518	N/D	0.00023	0.00018	0.05876	0.26552	0.14154	0.00002	0.75142	0.78224	0.08105
0.14980	0.10130	0.00000	0.00000	0.83220	0.00000	0.00000	0.00000	0.00000	0.04610	0.00000	0.00000	0.00000	0.00050

e given chemical element or oxide.

d to carry out the tests under consideration.

values)					
Dy	Ho	Er	Tm	Yb	Lu
0.50371	0.44466	0.24411	0.35292	0.77842	0.15132
0.95296	0.37400	0.37796	0.22069	0.20239	0.70845
0.70890	0.81224	0.08915	0.25342	0.86275	0.04013
0.00000	0.00000	0.00000	0.00000	0.00000	0.00000

Ce/Ce*	ΣREE	ΣLREE	ΣHREE	GRAIN-SIZE					
				< 4um	4-8 um	8-16 um	16-31 um	31-63 um	> 63 um
1.00	159.31	140.27	19.04	9.17	7.73	11.11	25.76	34.34	11.89
1.00	165.26	145.24	20.02	11.18	9.15	13.15	24.49	28.86	13.17
0.99	165.32	145.12	20.20	10.68	8.67	13.18	26.56	30.80	10.12
0.98	168.98	148.51	20.47	10.59	8.87	12.26	24.01	31.35	12.92
0.98	171.09	150.93	20.16	9.22	7.55	11.16	26.20	34.08	11.79
0.99	169.25	148.76	20.49	9.48	7.54	12.31	29.07	32.93	8.67
1.01	166.18	146.15	20.03	9.98	7.69	12.75	29.59	32.19	7.80
1.00	171.54	151.47	20.07	10.20	8.89	13.42	26.81	30.77	9.91
1.01	166.28	146.13	20.15	9.63	7.66	11.91	27.71	32.86	10.22
0.99	164.61	143.78	20.83	9.77	7.83	11.96	27.58	32.90	9.96
0.98	177.92	156.42	21.50	10.66	9.01	14.89	28.21	28.90	8.33
1.05	175.51	153.22	22.29	11.44	9.58	14.44	26.43	27.55	10.56
1.01	177.32	155.45	21.87	14.25	11.34	17.29	26.79	23.26	7.06
1.00	171.08	151.05	20.03	15.50	12.23	18.93	27.18	20.62	5.53
1.01	178.18	156.58	21.60	14.40	12.24	17.94	24.45	21.16	9.80
0.98	185.38	163.24	22.14	12.70	10.70	15.27	23.78	24.60	12.95
0.99	183.70	161.52	22.18	14.05	11.49	15.74	24.12	23.82	10.78
1.01	185.63	163.80	21.83	13.90	11.80	17.57	25.86	22.74	8.13
1.01	176.21	155.03	21.18	14.32	12.59	20.08	27.15	20.77	5.10
1.02	136.32	118.07	18.25	9.80	6.45	9.43	17.37	33.73	23.21
1.00	145.77	127.82	17.95	9.17	6.12	9.63	19.54	35.47	20.07
1.00	147.74	129.41	18.33	10.03	6.36	11.00	24.33	35.48	12.80
0.98	189.36	168.19	21.17	20.14	13.23	20.49	23.86	17.16	5.12
0.97	188.03	165.99	22.04	20.68	13.80	22.15	23.83	15.15	4.37
1.03	191.74	169.82	21.92	19.51	13.62	21.02	23.95	16.54	5.37
0.96	204.97	180.63	24.34	18.83	13.06	21.80	25.00	16.39	4.93
1.00	194.52	172.35	22.17	27.21	14.77	17.68	19.72	15.47	5.14
1.00	156.84	136.37	20.47	11.16	6.56	13.32	28.06	31.77	9.12
1.00	154.11	134.93	19.18	10.37	5.89	12.77	28.27	33.43	9.27
0.99	156.63	137.19	19.44	11.55	6.84	14.82	27.90	30.12	8.77
1.04	149.78	130.47	19.31	12.05	7.87	15.91	27.94	28.76	7.46
1.00	151.77	133.21	18.56	10.25	6.59	15.12	29.43	30.97	7.64
0.98	141.89	124.74	17.15	7.26	6.09	9.47	24.38	37.66	15.13
1.01	143.17	125.41	17.76	8.76	7.12	11.98	27.46	34.45	10.23
0.99	140.82	123.83	16.99	8.49	6.32	11.45	28.61	35.37	9.76
1.02	140.12	122.93	17.19	7.84	6.19	10.80	29.06	36.27	9.84
1.00	149.38	130.96	18.42	8.46	7.54	12.11	27.47	34.26	10.17
0.96	148.05	129.65	18.40	7.41	6.18	9.61	26.15	38.22	12.42
0.98	148.29	129.48	18.81	10.33	8.77	13.63	27.36	31.08	8.83
0.96	152.76	134.18	18.58	7.93	6.59	10.77	29.03	36.69	8.99
0.96	154.66	136.12	18.54	7.67	6.06	10.13	27.54	37.01	11.59
1.03	151.55	134.42	17.13	8.39	7.41	11.97	27.39	34.64	10.20
1.01	155.72	137.60	18.12	9.43	7.40	12.08	30.55	33.66	6.89
1.05	159.54	141.53	18.01	8.06	6.92	12.13	28.13	32.30	12.45
1.00	145.12	125.66	19.46	9.34	7.52	12.45	30.15	32.89	7.66
1.00	145.06	127.50	17.56	8.38	6.92	11.56	28.24	34.98	9.91
1.01	147.80	130.78	17.02	7.97	7.21	11.49	25.05	34.66	13.62
1.01	143.60	126.07	17.53	11.94	10.97	16.06	26.11	26.94	7.98
1.05	154.73	135.89	18.84	12.36	11.18	18.07	28.78	24.55	5.05
1.02	152.47	133.76	18.71	13.03	12.40	19.12	26.20	22.93	6.31
1.00	153.13	134.76	18.37	11.16	11.09	18.24	27.48	25.37	6.65
1.02	121.00	105.37	15.63	9.34	7.59	11.83	26.46	33.58	11.20
1.01	111.77	97.57	14.20	7.06	6.20	8.11	20.16	36.77	21.70
1.08	108.72	94.80	13.92	7.90	5.97	7.32	21.41	37.86	19.53
1.02	119.06	104.15	14.91	5.53	4.69	5.02	14.92	32.27	37.57
0.99	94.38	81.63	12.75	6.36	4.83	5.40	11.03	32.02	40.35
0.99	106.29	92.50	13.79	8.29	6.93	9.37	23.04	37.00	15.37
0.99	120.74	105.80	14.94	7.41	5.90	8.42	22.71	35.71	19.84
1.01	119.76	104.30	15.46	7.89	6.45	8.58	24.28	39.06	13.74
1.03	127.73	111.64	16.09	8.02	6.60	9.38	24.57	37.95	13.48
1.08	118.13	103.15	14.98	7.50	6.46	8.80	19.49	32.87	24.89
1.00	127.92	110.96	16.96	10.28	9.19	14.48	27.92	30.26	7.87
1.05	137.09	120.55	16.54	10.68	8.89	14.42	28.09	30.39	7.53
0.99	139.08	122.47	16.61	10.56	8.09	12.21	27.39	33.07	8.69

1.01	131.45	114.56	16.89	11.39	8.98	13.68	27.32	30.69	7.94
1.00	125.59	108.78	16.81	9.96	7.65	10.74	26.75	35.61	9.29
0.99	132.05	114.82	17.23	9.51	7.75	11.12	24.80	34.41	12.41
1.02	132.10	114.35	17.75	10.41	8.14	12.37	27.09	32.60	9.38
1.02	126.25	110.03	16.22	10.45	7.86	11.23	26.38	34.09	9.98
1.00	131.77	114.60	17.17	11.37	8.39	13.72	29.05	30.69	6.79
1.03	140.07	122.85	17.22	11.34	8.99	13.10	26.62	31.39	8.55
1.01	128.96	112.52	16.44	11.55	9.19	16.18	32.00	27.64	3.45
1.01	135.08	118.58	16.50	14.18	11.59	20.26	31.33	20.56	2.09
1.00	131.46	114.79	16.67	11.96	9.64	17.49	32.63	25.63	2.66
0.98	130.28	114.52	15.76	9.30	6.95	9.24	27.90	37.85	8.77
1.02	153.98	134.78	19.20	9.48	7.71	10.56	25.51	35.64	11.10
1.01	141.75	123.26	18.49	12.55	10.03	14.21	27.36	29.06	6.79
1.02	144.33	126.87	17.46	12.69	10.39	15.21	27.99	27.76	5.96
1.02	139.67	121.73	17.94	12.10	9.93	15.48	29.25	27.73	5.51
1.04	143.19	126.15	17.04	13.35	11.36	15.77	27.24	26.46	5.82
1.01	138.36	121.26	17.10	15.73	12.43	18.63	28.31	21.63	3.27
1.02	141.70	124.71	16.99	16.22	13.30	18.63	27.04	21.14	3.67
1.02	151.92	134.24	17.68	15.05	14.38	22.30	26.92	18.06	3.29
1.02	142.79	124.86	17.93	9.38	7.98	12.68	28.18	33.82	7.98
1.01	143.35	125.70	17.65	9.06	7.47	12.51	28.72	34.28	7.96
0.98	147.90	129.51	18.39	10.92	8.43	12.25	27.65	33.08	7.67
1.02	142.64	124.51	18.13	10.24	8.13	13.27	29.12	32.38	6.87
1.00	152.85	132.86	19.99	10.69	8.83	13.59	28.18	31.72	6.99
0.97	155.34	135.66	19.68	9.79	8.18	11.99	27.41	34.35	8.28

Ce/Ce*	ΣREE	ΣLREE	ΣHREE	GRAIN-SIZE					
				< 4um	4-8 um	8-16 um	16-31 um	31-63 um	> 63 um
1.00	171.09	151.05	20.49	10.68	9.01	13.42	26.56	28.90	9.96
1.00	148.29	130.78	18.12	8.46	7.21	11.98	27.48	34.45	9.84
1.01	131.46	114.54	16.64	10.43	8.12	12.29	26.98	32.15	8.73
1.00	145.77	127.82	18.25	9.80	6.36	9.63	19.54	35.47	20.07
0.98	191.74	169.82	22.04	20.14	13.62	21.02	23.86	16.39	5.12
1.00	154.11	134.93	19.31	11.16	6.59	14.82	28.06	30.97	8.77
1.00	145.63	127.61	18.26	10.01	8.16	12.59	28.18	33.45	7.81
1.00	172.57	151.72	20.85	11.64	9.61	14.49	26.41	28.13	9.72
1.00	148.83	130.80	18.03	9.17	7.89	12.80	27.64	32.84	9.67
1.02	129.74	113.38	16.35	10.48	8.51	12.60	25.72	31.17	11.52
1.00	143.28	125.10	18.18	9.67	6.31	10.02	20.41	34.89	18.69
0.99	193.72	171.40	22.33	21.27	13.70	20.63	23.27	16.14	4.99
1.01	153.83	134.43	19.39	11.08	6.75	14.39	28.32	31.01	8.45
1.00	147.48	128.85	18.63	10.01	8.17	12.71	28.21	33.27	7.62
0.98	159.31	140.27	19.04	9.17	7.54	11.11	23.78	20.62	5.10
0.96	140.12	122.93	16.99	7.26	6.06	9.47	24.38	22.93	5.05
0.98	94.38	81.63	12.75	5.53	4.69	5.02	11.03	18.06	2.09
1.00	136.32	118.07	17.95	9.17	6.12	9.43	17.37	33.73	12.80
0.96	188.03	165.99	21.17	18.83	13.06	17.68	19.72	15.15	4.37
0.99	149.78	130.47	18.56	10.25	5.89	12.77	27.90	28.76	7.46
0.97	142.64	124.51	17.65	9.06	7.47	11.99	27.41	31.72	6.87
1.05	185.63	163.80	22.29	15.50	12.59	20.08	29.59	34.34	13.17
1.05	159.54	141.53	19.46	13.03	12.40	19.12	30.55	38.22	15.13
1.08	153.98	134.78	19.20	16.22	14.38	22.30	32.63	39.06	40.35
1.02	147.74	129.41	18.33	10.03	6.45	11.00	24.33	35.48	23.21
1.03	204.97	180.63	24.34	27.21	14.77	22.15	25.00	17.16	5.37
1.04	156.84	137.19	20.47	12.05	7.87	15.91	29.43	33.43	9.27
1.02	155.34	135.66	19.99	10.92	8.83	13.59	29.12	34.35	8.28
0.02	7.32	6.53	0.92	2.06	1.78	2.67	1.64	4.74	2.28
0.03	5.45	5.15	0.71	1.71	1.94	2.84	1.55	4.47	2.54
0.02	12.92	11.63	1.40	2.63	2.29	4.14	4.43	5.39	9.02
0.01	4.98	5.01	0.16	0.36	0.14	0.70	2.91	0.82	4.36
0.02	6.04	5.06	1.06	3.03	0.60	1.58	1.83	0.73	0.34
0.02	2.74	2.40	0.62	0.69	0.64	1.17	0.57	1.57	0.76
0.02	5.05	4.23	0.89	0.67	0.42	0.56	0.58	0.98	0.52
1.00	147.90	129.51	18.25	10.33	7.98	12.75	27.18	32.19	8.83
1.01	149.56	131.17	18.39	11.03	8.71	13.52	26.27	30.29	10.18
0.96	94.38	81.63	12.75	5.53	4.69	5.02	11.03	15.15	2.09
1.08	204.97	180.63	24.34	27.21	14.77	22.30	32.63	39.06	40.35
0.02	21.20	19.09	2.21	3.40	2.36	3.69	3.37	5.92	6.14

